We would like to thank the reviewers and the Editor for their careful re-review of our manuscript. Our point-by-point responses to all the comments and annotations are presented below. The comments from the reviewer are shown in black, and our responses in red. Where indicated, additions to the manuscript are shown in blue and deleted text is indicated by red strikethrough, and line numbers are based on our revised (non-track) manuscript. Besides, we added some information about changes in the paper that are not mentioned in the response to the Reviewers They are following:

1. We corrected the Figures 2, 3, 8 (previous № 6) replacing «км» to «km» at the scale bar and the Figures 5,6 (previous № 7) with «Kyr» corrected to «kyr»

2. We corrected the Fig. 7 (previous № 8) and it's caption to align with the text

==========

Referee #2

Comments from the reviewer #2 and our responses:

Major comments:

Comment

1. Lines 89-93: I am afraid the following is not easily reproducible by other researchers: "Then the modeling results were extrapolated to complex sections that comprise alternating reference lithologies or different combinations of relatively thick layers. We consider two cases to extrapolate our results: In the first case, we consider the uniform alternation of homogeneous layers with a relatively low thickness (relative to the total thickness of the permafrost). The linear interpolation is simply performed in accordance with the percentage of the thickness of frozen ground obtained during modeling for two —pure soils at a given moment." Please make a more precise and explicit description and verification of the proposed procedure. Details could be added to the supplemental material

Response

→ We added the detailed description of the method we used to extrapolate the results of the modeling to the different kinds of sections

→ Lines 101-102:

→ Therefore, as a first approximation, this change is linear (which is not entirely true) and a simple linear interpolation formula can be obtained (Supplement 1).

→

Supplement 1. Extrapolation of the modeling results of permafrost thickness to real geological sections.

Carrying out such a procedure is necessary to reduce the number of simulated thermal tasks to a reasonable limit. There are several approaches.

A. In the first case, we consider the uniform alternation of homogeneous layers with a relatively low thickness (relative to the total thickness of the permafrost). The linear interpolation is simply performed in accordance with the percentage of the thickness of frozen ground obtained during modeling for two "pure" soils at a given moment.

There are 2 options here:

1. We have the thicknesses of frozen layers in sand (T_s) and loam (T_l) (clay) sediments from the simulation in similar conditions (scenario, heat flux). Then the formula will be:

$$T_{al} = T_l + n_s * (T_s - T_l), (1)$$

where n_s is the relative content of sand layers in the section

The same formula can also be used to evaluate the thawing of permafrost from above, if this occurs in accordance with a specific scenario

2. More complicated is the very common case when, for example, relict permafrost is preserved in sandy sediments within the water area, and in loam it thaws completely long before modern times.

In this case, we apply the following approximate approach.

For a reference soil in which frozen soils are not preserved up to the present (and this is always loam (clay) in the considered pair of reference soils), the last point of the existence of permafrost at the τ_{deg} (time of degradation) is found at the corresponding graph. This point, in the absence of thawing from above, is located on the surface, otherwise, at a certain depth from the bottom z_{deg}, where the upper and lower fronts of thawing of permafrost in the loams meet.

At this point, according to the slope of curve representing the movement of the base of permafrost, the rate of thawing ν_{th} from below is determined right before the complete disappearance of the frozen layer. Based on this rate of the upward movement of the lower boundary of the permafrost, the value of the potential thawing of loams from the moment τ_{deg} is calculated:

$$\xi_{lb} = \nu_{\text{th}} \times \tau_{\text{deg}} \quad (2)$$

and the estimated (fictitious) position of the modern lower permafrost boundary in the loamy rocks relative to the bottom surface will be equal to

$$T_{lb}^{f} = z_{\text{deg}} - \xi_{lb} \quad (3)$$

The value T_{lb}^{f} can be either positive (below the bottom) or negative (above the bottom).

Putting T_{lb}^{f} in (1) instead of Tc allows to find the position of the lower boundary T_{al} of frozen soils in a layered sandy-loamy section with a given relative content of sand layers (n_s). A negative value clearly indicates the complete degradation of permafrost so far even in the absence of thawing from above.

To obtain the thawing from above for the alternating layers of sediments, the following approximate approach is used. At the moment of the complete degradation of frozen loams τ_{deg}, according to the graph of permafrost dynamics, the thawing value from above $\xi_{ub}(\tau_{\text{deg}})$ is found for sandy soil and the ratio

$p = z_{\text{deg}}/\xi_{ub}(\tau_{\text{deg}})$ is calculated. It is assumed that the indicated ratio of thawing depths from above for soils of different compositions at the time of permafrost degradation in loamy sediments is preserved up to the present. Then the potential thawing on top of the loams at the moment will be

$$\xi_{ub}^{m} = p \times \xi_{ub} \quad (4),$$

where ξ_{ub}^{m} and ξ_{ub} are the calculated depth of thawing from the top for the loams and the model depth of thawing from the top for the sand accordingly, to the current time

The current position of the permafrost top under the sea floor ξ_m for a layered section of bottom sediments with a given relative content of sand (n_s) is found from a dependence of type (1), which in this case has the next form:

$$\xi_m = \xi_{ub}^{m} + n_s \times (\xi_{ub} - \xi_{ub}^{m}) \quad (5)$$

Next, the residual thickness of the layered permafrost under the sea bottom should be found.

$$th_{res} = T_{al} - \xi_m \quad (6)$$

If the value $th_{res} < 0$ then the relict permafrost do not persist at a specific point in the water area.

B. Extrapolation of simulation results of submarine permafrost in homogeneous soils into a two-layer geological section.

The case is considered when the thickness of the sediments is relatively small and bedrock lies from a shallow depth under the bottom. An approximate approach is known to estimate the freezing depth of a two-layer strate with known freezing depths of the rocks of the upper and lower layers separately, all other things being equal.

This approach is based on obvious points. At zero thickness of the upper layer of sediments (th_1=0), freezing of a two-layer system is equal to freezing in the lower layer $\xi_{2l} = \xi_l$, and at a thickness of the upper layer equal to the depth of freezing of the upper layer ($th_1 = \xi_u$) freezing of the system is equal to freezing of the upper layer $\xi_{2l} = \xi_u$.
Intermediate freezing depths of this two-layered system for random values of the upper layer thickness are considered varying linearly between these extreme values, where the following relationship is obtained.

$$\xi_{2l} = \xi_l + (1 - \frac{\xi_l}{\xi_u}) \times th_1 \quad (7)$$

It is clear that the limits of variation in the thickness of the upper layer of ground are limited – when $th_1 > \xi_u$ the system becomes single-layer. Equation (7) is valid as well for thawing of the permafrost for two-layer structure section.
There are also two cases of interpolation.
1. The modern thickness of permafrost in sediments (Th_{sed}) and bedrocks (Th_{br}), is obtained under the same other conditions (scenario, heat flow) from the simulation results. Then the formula for determining the thickness of permafrost in a two-layer system will obviously have the next form:

$$Th_{2l} = Th_{br} + \left(1 - \frac{Th_{br}}{Th_{sed}}\right) \times th_1,$$

where th_1 is the thickness of the upper layer of sediments or the depth of the top of the bedrocks. We consider the sediments as the strata of alternating sand and loam with a given ratio in the section. The extrapolation of modeling results of homogeneous reference soils to a layered stratum was considered in the previous section.
The same dependence can also be used to evaluate thawing of two-layer permafrost from above.
2. Often there is a situation when the relict permafrost is preserved in sediments but in rocky deposits it is completely degraded to the current moment. In this situation, the same approach is used as previously considered (see section A). Using data on the depth and period of complete thawing of permafrost in bedrocks as well as on the dynamics of the movement of thawing fronts immediately before the disappearance of frozen rocks, the calculated (fictitious) position of the boundaries of frozen rocks at the modern time is determined using the dependencies (2-4), and the prediction of thawing of frozen rock from above is carried out according to (4) using the dynamics of sandy permafrost.
Using the same methodology, the fictitious positions of the upper and lower boundaries of the permafrost in sediments are calculated - i.e. layered strata with a given relative sand content. Further, substituting the obtained fictitious positions of the permafrost boundaries in sediments and rocks in (8), we find the position of these boundaries in a two-layer section. The current residual thickness of the permafrost is necessarily calculated as the difference in the depths of the positions of their lower and upper boundaries - a negative sign of this value indicates degradation of shelf permafrost.

Comment

2. 2. I could not find where the initial ground temperature distribution is given in the manuscript. The newly provided supplement indicates that the ground was thawed (no permafrost). Why was it assumed so? How would the modeling results differ if some permafrost was preserved 120kya?

Response

→ The initial distribution of ground temperatures is presented not only at the added figure. It is reflected in fig. 5 and 7 (current № 6), as a result of the existence of a marine warm-water basin transgressing to the continental coastal plains in MIS-5e (Map of Quaternary Formations of the Russian Federation (Zastrozhnov et al.), 2014; Astakhov and Nazarov, 2010; Gusev et al.,

2016). This basin began to form long before the MIS-5e optimum - about 140 kyr BP (Astakhov and Nazarov, 2010). The authors provided preleminary modeling for 200-117 kyr BP that showed the thawing of permafrost that had been formed before MIS-5e under the sea, which had existed for more than 20 kyr, as well as stabilization of the thermal field of ground. These results are consistent with the previously obtained ideas about the thawing of permafrost under the MIS-5e sea within the north of Western Siberia (Baulin, 1979; 1985). It was thicker permafrost since it was formed under more severe subaerial conditions and during longer period, but it was thawed. Therefore, there were no prerequisites for giving the existence of permafrost in MIS-5e. Still, if the existence of permafrost in MIS-5e was nevertheless given, it (existence) is unlikely to change the results obtained in this study. The frozen ground in MIS-5e and others formed before MIS-3 most likely had been thawed under the sea that existed in MIS-3 for 25 thousand years. The result would remain the same.

→ The next sentences were added (Lines 241-245):

→ The initial conditions are those given for the interglacial MIS-5e . There was a warm-water sea basin on the Kara shelf and adjacent lowlands from 140 to 117 kyr (Fig. 5, 6) (Astakhov and Nazarov, 2010; Nazarov, 2011; Gusev et al., 2016a). Preliminary modeling for the interval MIS-6 - MIS-5e (200-117 kyr BP) showed that previously formed permafrost completely thawed under the sea during MIS-5e, which had existed for more than 20 kyr.The sequence of paleogeographic events in the form of a series of cartographic schemes is shown in Fig. 7.

→ The sentence was moved further from Line 229 to Line 260 (right after Fig.7)

→ .~~Altogether thirty such curves have been obtained, each based on four lithological patterns and two heat flux values.~~

Altogether thirty curves have been obtained, each based on four lithological patterns and two heat flux values.

→ The next sentence was added (Lines 260-262):

~~During transgressions in the Holocene~~ An important role in the formation of the current permafrost is the last (Holocene) transgression of the sea. Therefore, it was set that~~,~~ that each shelf part stayed for 400-2000 years in the coastal zone where bottom sediments were flooded with saline and warm near-bottom water. It is known that at sea depths from 2 to 7 m in the 1970s (Zhigarev, 1981), up to 10 m in the 2000s.

Minor comments:

Comment

1. Line 79: Please provide a reference to “the explicit two-layer scheme“
2. Line 79: Please provide a reference to “the balance method”

Response

We added the reference to the text and References (Lines 78-79 and Lines 642-643):

→ The explicit two-layer scheme is applied using the balance method (Pustovoit, G.P, 1999) and the enthalpy formulation of the problem.

→ Pustovoit, G.P.: Numerical solutions / Fundamentals of Geocryology. Part 5. (Engineering geocryology), edited by: Ershov, E. D., Moscow State University, Moscow, 41-55, 1999 (in Russian).

Comment

3. Please try to combine figures 5 and 7. I think it would be reasonable thing to do.

Response

→ The comment is right. We agree with the reviewer. The figure 7 is moved upper (it's № 6 now). The fig. 6 (it's № 8 now) is moved to the end of the Paleogeographic scenarios section. In current version the illustrations on paleotemperature curves follow one another. Besides, we made changes in the captions to drawings in order to have it more uniform.

→ Lines 247-249:

→ Fig. 5. Paleotemperature curves for the periglacial subaerial part of the shelf:
1 = southwestern shelf part (SW), 80 m isobath; 2 = southwestern shelf part (SW), 5 m isobath;
3 = northeastern shelf part (NE), 120 m isobath.

→ Lines 250-252

→ Fig.67. ~~Paleogeographic scenario~~ Paleo-temperature curves for 50 m isobath :~~for MIS-2 which controlled the present distribution of frozen and cooled ground. Adapted for modeling purposes. A fragment.~~
1 = periglacial subaerial northeastern shelf part (**NE**); 2 = ice that reached the bottom for 7-10 kyr, **G-1**); 3 = subaqual (beneath damlake) central shelf part, **C**;

Comment
4. Move figure 8 close to the introduction, prior to the development of the paleo scenarios.

Response
→ We moved Fig. 8 right after the Fig.5 and 6. It's current number is 7. Unfortunately, according to the logic of the article, we do not see the way of moving the figure closer to the introduction

Comment
5. Move figure 6 closer to the introduction as well. Modeling results should not be combined with the data driven figures. You provided a good justification for assuming a salt contaminated ground across the modeling domain in the responses to the reviewers. Please copy-paste it to the manuscript, in the current copy of the manuscript it is still a rather cryptic note.

Response
→ Unfortunately, according to the logic of the article, we do not see the way of moving the figure closer to the introduction

→ We added the text and the reference from the previous responses to the reviewers (Lines 103-114 and 539-541).

→ All reference rocks and sediments were considered saline with Ds = 0.8-1.1% according to the concentration of pore saline solution corresponding to that of Kara sea bottom waters concentration (32-34 ‰). The freezing temperature equal to the freezing temperature of sea water (- 1,8°C) was set for all types of soils for the modeling. This assumption was made due to the fact that all the marine sediments composing the Yamal Peninsula have the close values of the salinity to a depth of 300 m and more (Chuvilin et al., 2007).Very high degree of averaging over the properties was used for the modeling caused by the lack of data on the water area. The rare drilling data showed the salinization of sediments through the entire drilling depth. So there was not possible to take into account the salt diffusion, and the salinity did not vary with the depth. Because the modeling has evaluative nature a scheme with complete freezing (thawing) of moisture in the ground at the moving front of phase transitions was used. The content of unfrozen water in the sediments was taken into account by reducing the volumetric heat of phase transitions in the model by the value corresponding to the average content of unfrozen water in different types of rocks at negative temperatures typical of the process under study (Chuvilin et al., 2007).~~Therefore the freezing temperature of the pore solution is close to -1.8 °C.~~

→ Chuvilin, E.M., Perlova, E.V., Baranov, Yu.B., Kondakov, V.V., Osokin, A.B., Yakushev, V.S.: The structure and properties of cryolithozone sediments of the southern part of the Bovanenkovo gas condensate field. Geos, Moscow, 20, 2007 (in Russian).

Comment

6. Mark locations of the map that correspond to the scenarios in Figures 5 and 7

Response

→ In the figure captions there is an indication that the curves refer to certain isobaths. However, only the main ones (100, 200) are presented on the given fragment of the geocryological map. They give an idea of the location of the curves. Unfortunately, we do not see the possibility of otherwise expressing it. For greater clarity, we have added the 50m isobath to the map.

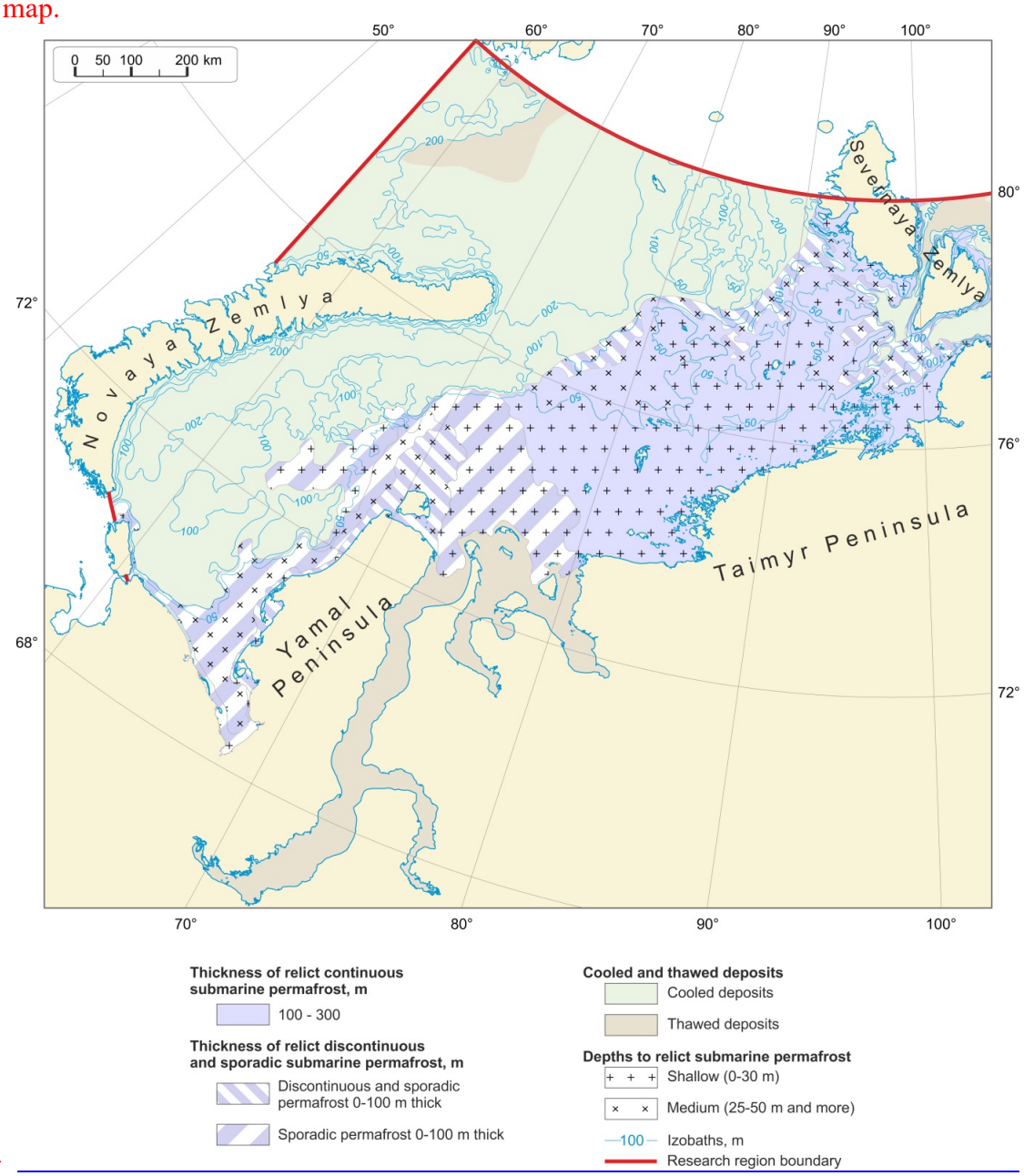

→

Comment

7. In Table 1, add years when the ice-dammed lake existed.

→ The dammed basins existed when the MIS-2 glacier existed. We have set it from 25 to 15 kyr. We added this information to the Table 1

Domains	Subdomains	Areas (landscapes)		Subareas
Periglacial domain	Subaerial	Southwestern shelf	**SW**	Sea depths 0-120 m (contour intervals of average depths at 5, 20, 50, 80 and 100 m)
		Northeastern shelf	**NE**	
	Subaqual (under ice-dammed lake) for 25-15 кyr	Central shelf	**C**	Sea depths 0-80 m
		Estuaries	**E**	
Glacial domain, ice reaching sea bottom	Subaqual (for 7-10 kyr)	**G-1**		Sea depths 0-200 m
Glacial domain, shelf ice, MIS-2	Subglacial-subaqual	**G-2**		Sea depths 200-800 m

The Current State and 125 kyr History of Permafrost in the Kara Sea Shelf: Modeling Constraints

Anatoliy Gavrilov [1,3], Vladimir Pavlov [4], Alexandr Fridenberg [4], Mikhail Boldyrev [5], Vanda Khilimonyuk [1,3], Elena Pizhankova [1,3], Sergey Buldovich [1,3], Natalia Kosevich [1,3], Ali Alyautdinov [2,3], Mariia Ogienko [1,3], Alexander Roslyakov [1,3], Maria Cherbunina [1,3], Evgeniy Ospennikov [1,3].

[1] Lomonosov Moscow State University, Geological faculty, Moscow, Russia

[2] Lomonosov Moscow State University, Geographic faculty, Moscow, Russia

[3] Foundation «National Intellectual Resource», Moscow, Russia

[4] Rosneft Oil Company, Moscow, Russia

[5] LLC «Arctic Research Center», Moscow, Russia

Abstract. The evolution of permafrost in the Kara shelf is reconstructed for the past 125 kyr. The work includes zoning of the shelf according to geological history, compiling sea level and ground temperature scenarios within the distinguished zones, and modeling to evaluate the thickness of permafrost and the distribution of frozen, cooled and thawed deposits. Special attention is given to the scenarios of the evolution of ground temperature in key stages of history that determined the current state of the Kara shelf permafrost zone: characterization of the extensiveness and duration of the existence of the sea during the marine isotope stage MIS -3, the spread of glaciation and dammed basins in MIS-2. The present shelf is divided into areas of continuous, discontinuous to sporadic, and sporadic permafrost. Cooled deposits occur at west and northwest water zone and correspond to areas of MIS-2 glaciation. Permafrost occurs in the periglacial domain that is a zone of modern sea depth from 0 to 100 m, adjacent to the continent. The distribution of permafrost is mostly sporadic in the southwest of this zone, while it is mostly continuous in the northeast. The thickness of permafrost does not exceed 100 m in the southeast , and ranges from 100 to 300 m in the northeast. Thawed deposits are confined to the estuaries of large rivers and the deepwater part of the St. Anna trench. The modeling results are correlated to the available field data and are presented as geocryological maps. The formation of frozen, cooled and thawed deposits of the region is inferred to depend on the spread of ice sheets, sea level, and duration of shelf freezing and thawing periods.

1. Introduction

Permafrost studies and mapping in the Kara Sea shelf (Fig. 1) have a long history. The first evidence of its distribution in the Kara and other Eurasian Arctic shelves appeared in early permafrost maps of the USSR (Parkhomenko, 1937; Baranov, 1960). The distribution and approximate thickness of the Kara shelf permafrost were first calculated numerically in the early 1970s (Chekhovsky, 1972). By late 1970s - early 1980s, Soloviev and Neizvestnov mapped the whole Russian shelf, and their work became part of the later 1:2 500 000 Geocryological Map of the USSR (Yershov, 1991). The dynamics of subsea permafrost in the Kara shelf during regression and transgression events was reconstructed by modeling (Danilov and Buldovich, 2001). Drilling was first used to study the features of permafrost and its recent formation in the near-shore zone of the Yamal Peninsula (Grigoriev, 1987).

Since 1986, drilling and seismoacoustic surveys have been run by the Arctic Marine Engineering Geological Survey (AMEGS) to constrain the extent of the Kara shelf permafrost and the depths to its top and base; the results were reported in a number of publications (Melnikov and Spesivtsev, 1995; Dlugach and Antonenko, 1996; Bondarev et al., 2001; Rokos et al., 2009; Kulikov and Rokos, 2017; Vasilyev et al., 2018). However, the available data are restricted to the southwestern part of the shelf while the more severe northeastern part remains poorly documented and undrilled.

Another recent map of permafrost distribution and thickness in the southwestern Kara shelf (Portnov et al., 2013) is based on seismoacoustic data and modeling with reference to the glacial eustatic curve but without regard to regional features related to the existence of MIS-3 marine terraces. Followed by drilling and seismoacoustic results from the western Yamal Peninsula shelf (Melnikov and Spesivtsev, 1995; Dlugach and Antonenko, 1996; Baulin 2001; Baulin et al., 2005; etc.), geocryological modeling has become quite realistic lately, but its quality is still insufficient for economic activity, even within the best documented southwestern Kara shelf. As for the northeastern and central shelf parts, the knowledge is very preliminary.

The available permafrost maps refer to the isobaths ofthe maximum regression during the peak of cold stage 2 of the marine oxygen isotope stratigraphy (MIS-2). This reference is yet uncertain because the sea depths and level apparently varied in a range of at least tens of meters during the Late Pleistocene-Holocene glaciation history and related isostatic movements, as one may infer from the elevations of MIS-4 and MIS-3 marine terraces in Novaya Zemlya Islands which are

raised high (+45, +55,+60 m, Bolsiyanov et al., 2006) and the adjacent continent (Yamal, Gydan) terraces on which were formed at low sea level (-100 and -70 m respectively, Siddall et al., 2003; 2006)

Given the logistic challenge and high costs of field studies, the knowledge of the Kara shelf permafrost can be extended by numerical modeling. Its application makes it possible to establish the connection of permafrost with components of the natural environment, including glaciations, glacio-isostatic movements and fluctuations in sea level.

2. Research methodology and its implementation

Permafrost in the Arctic shelf is mostly of relict origin: it formed during regressions and cold climate events and then degraded during Late Pleistocene-Holocene transgressions.

The methods for subsea permafrost research have been developed since the 1970s and use the retrospective approach of reconstructing the permafrost evolution (Gavrilov, 2008; Romanovsky and Tumskoi, 2011). The history of methods applied to study the structure and t distribution of permafrost of the eastern Russian Arctic was reviewed previously (Gavrilov et al., 2001; Gavrilov, 2008; Nicolsky et al., 2012). We follow these methods in our research and are trying to extend their work . The work includes compiling a database of paleogeographic, geological, tectonic, and geocryological conditions used further to divide the region according to geological history and for creating possible scenarios of sea level and ground temperature variations that serve as boundary conditions in heat transfer modeling. The general scheme of the methodology is presented in Figure 1.

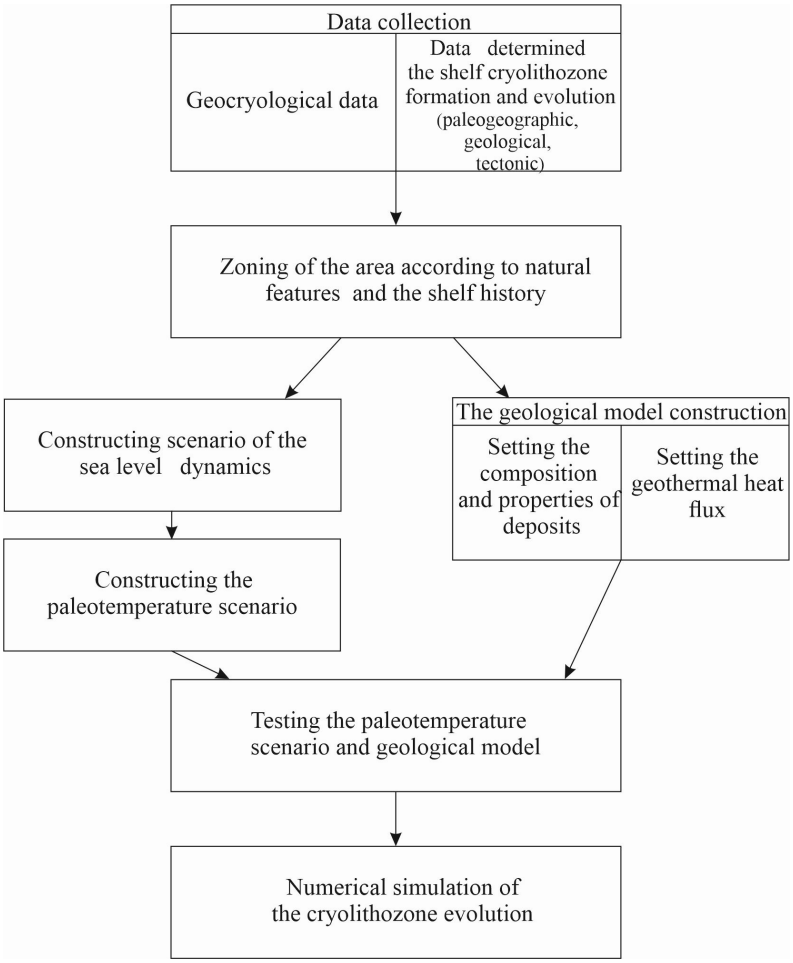

Fig. 1. The general scheme of the methodology.

The zoning is determined by the allocation of territorial units that are characterized by uniformity of formation conditions and, accordingly, by similar (on the given scale of the studies) parameters of permafrost: its distribution, thickness, depths of the top (Kudryavtsev, 1979).The history of subsea permafrost has been modeled using software designed at the Department of Geocryology of the Geological Faculty in the Moscow State University (Khrustalev et al., 1994; Pesotsky, 2016). The software can solve Stefan's problems for non-steady state thermal conductivity assuming moving fronts of pore moisture phase transitions within the modeling domain and variable boundary conditions. The explicit two-layer scheme is applied using the balance method (Pustovoit, G.P, 1999) and the enthalpy formulation of the problem. The code used is publicly available under https://github.com/kriolog/qfrost (last access: 15 February 2020) (kriolog, 2020).

The permafrost dynamics was simulated for numerous paleoclimate scenarios that cover the full range of presumable conditions in the Arctic shelves.. The total number of paleo-scenarios for the Kara sea used in the course of mathematical modeling was 30 .The 1D modeling domain had a vertical size of 5 km to avoid the effect of its base on the permafrost dynamics. The temperatures at the surface according to the available paleoclimate reconstructions and a heat flux at the base of the modeling domain were used as the first- and second order boundary conditions, respectively. The heat flux was assumed to be 50 mW/m2 , which corresponds to the average for most of the shelf territory or 75 mW/m2, as in zones of relatively high heat flux in gas-bearing bottom sediments (Khutorskoy et al., 2013).The modeling was performed for several uniform reference rock and sediment types in order to reduce the number of possible solutions in the conditions of high lithological diversity in the area. Then the modeling results were extrapolated to complex sections that comprise alternating reference lithologies or different combinations of relatively thick layers. We consider two cases to extrapolate our results:In the first case, we consider the uniform alternation of homogeneous layers with a relatively low thickness (relative to the total thickness of the permafrost). The linear interpolation is simply performed in accordance with the percentage of the thickness of frozen ground obtained during modeling for two "pure" soils at a given moment.The second case relates to the two-layer structure of the section, when a sufficiently thick (as compared with the permafrost thickness) homogeneous layer is underlained by a second homogeneous layer of unlimited thickness. Then the following considerations are valid. If the thickness of the upper layer is zero, then the thickness of the permafrost is equal to the result of simulation for "pure" rocks/sediments of the second layer. If the thickness of the upper layer is equal to (or more) the thickness of the permafrost obtained for the first layer, then the problem becomes single-layer and the thickness of the permafrost is equal to that of the first layer. Therefore, when the thickness of the upper layer changes from zero to the thickness of the permafrost of the first layer, the thickness of the two-layer section changes from the thickness of the permafrost of the second layer to the permafrost thickness the first layer. Therefore, as a first approximation, this change is linear (which is not entirely true) and a simple linear interpolation formula can be obtained (Supplement 1)..All deposits were assumed to be saline from top to bottom of the modeling domain .All reference rocks and sediments were considered saline with Ds = 0.8-1.1% according to the concentration of pore saline solution corresponding to that of Kara sea bottom waters concentration (32-34 ‰). The freezing temperature equal to the freezing temperature of sea water (- 1,8°C) was set for all types of soils for the modeling. This assumption was made due to the fact that all the marine sediments composing the Yamal Peninsula have the close values of the salinity to a depth of 300 m and more . Very high degree of averaging over the properties was used for the modeling caused by the lack of data on the water area. The rare drilling data showed the salinization of sediments through the entire drilling depth. So there was not possible to take into account the salt diffusion, and the salinity did not vary with the depth. Because the modeling has evaluative nature a scheme with complete freezing (thawing) of moisture in the ground at the moving front of phase transitions was used. The content of unfrozen water in the sediments was taken into account by reducing the volumetric heat of phase transitions in the model by the value corresponding to the average content of unfrozen water in different types of rocks at negative temperatures typical of the process under study (Chuvilin et al., 2007). ~~Therefore the freezing temperature of the pore solution is close to -1.8 °C.~~

Thermophysical properties, the content of unfrozen water and the heat of the phase transitions of water in the pores, the freezing point of the deposits were set taking into account the indicated salinization. The paleotemperature scenarios and the geological-tectonic model were tested by comparing the present permafrost state estimated by forward modeling with the available field data from well documented areas, to achieve the best fit.

The evolution of the shelf permafrost was reconstructed by heat transfer modeling for the Late Pleistocene-Holocene, since 125 kyr, the end of a long-term interglacial transgression. At that time, subsea permafrost had presumably fully degraded over the whole studied part of the Kara Sea,as the entire north of the West Siberian Plain had been covered by the sea from 140 to 120 Ka (Zastorozhnov et al., 2010; Shishkin et al., 2015) and the temperatures of unfrozen bottom sediments approached the steady state. The modeling results were correlated with field data and both datasets were used for the final geocryological zoning of the Kara shelf region. The Kara shelf has been quite well studied in terms of paleogeography. Figure 2 compiles the various studies available for the paleogeography of this region.

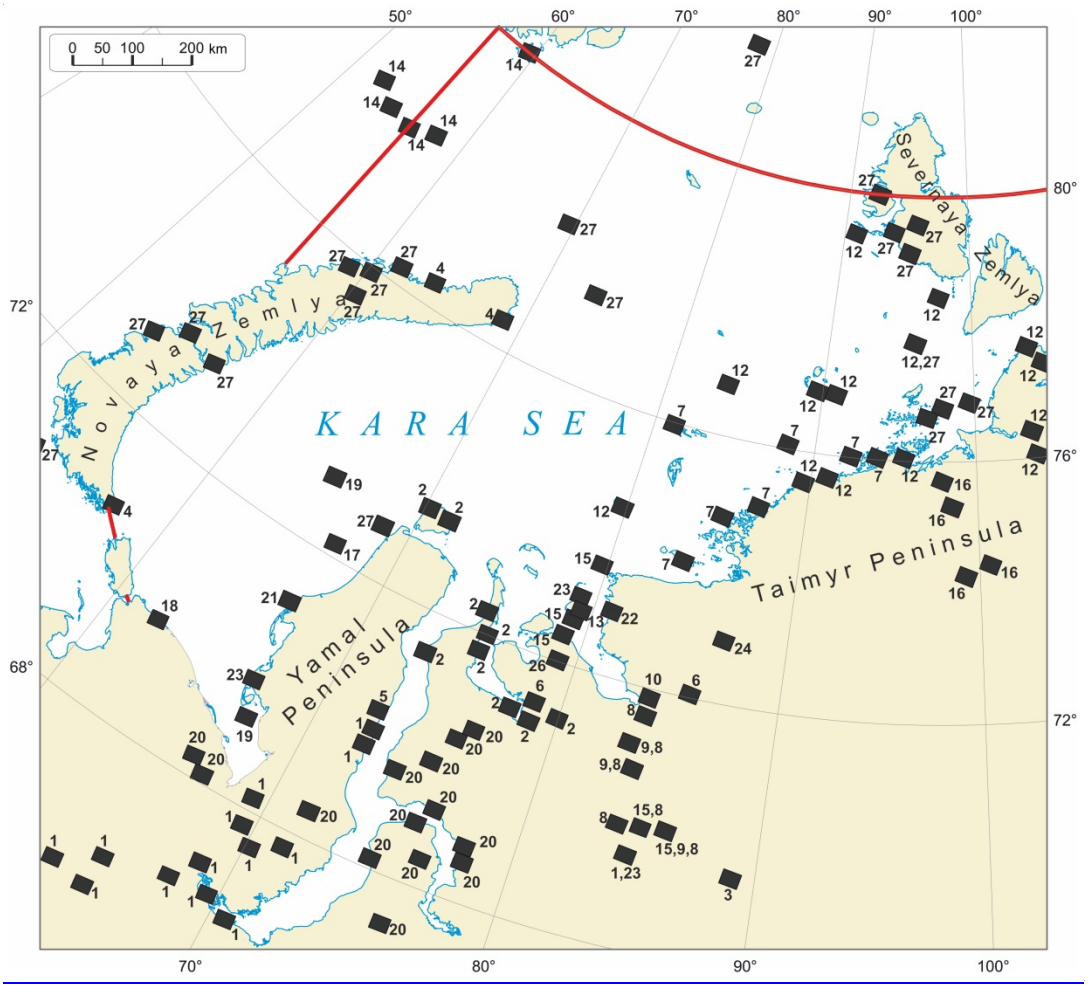

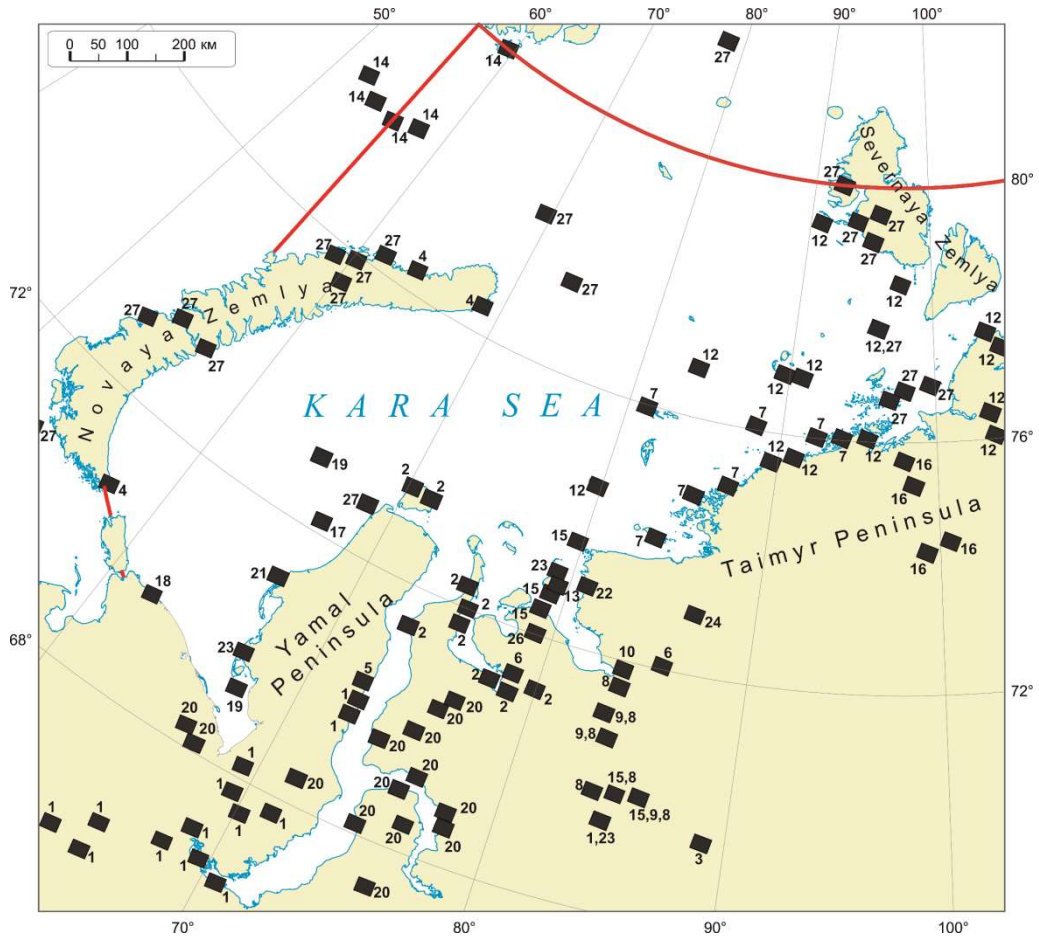

Fig. 2. Late Pleistocene geology of the Kara region: data coverage (the red line is the research region boundary). The numbers on the map correspond to the following publications:

Black squares are sites studied in different years by different research teams. Numbers 1 to 28 refer to publications: 1 = Astakhov and Nazarov (2010); 2 = Baranskaya et al. (2018); 3 = Bolshiyanov et al. (2007); 4 = Bolshiyanov et al. (2009); 5 = Vasil`chuk (1992); 6 = Geinz and Garutt (1964); 7 = Gusev et al. (2016a); 8 = Gusev et al. (2016b); 9 = Gusev et al. (2015a); 10 = Gusev et al. (2015b); 11 = Gusev et al. (2013); 12 = Gusev et al. (2012a); 13 = Gusev and Molod`kov (2012); 14 = Gusev et al. (2012b); 15 = Gusev et al. (2011); 16 = Derevyagin et al. (1999); 17 = Kulikov and Rokos (2017); 18 = Leibman and Kizyakov (2007); 19 = Melnikov and Spesivtsev (1995); 20 = Nazarov (2011); 21 = Grigoriev (1987); 22 = Streletskaya et al. (2012); 23 = Streletskaya et al. (2015); 24 = Sulerzhitsky et al. (1995); 25 = Forman et al. (2002); 26 = Gilbert et al. (2007); 27 = Hughes et al. (2016); 28 = Svendsen et al. (2004).

3. Paleogeographic scenarios

There is number of ideas about the paleogeography of the Kara region and its development in the Late Pleistocene. Evaluation of the validity of these ideas and the selection of the most reasonable of them was one of the objectives of the present studies. The most popular are two controversial hypotheses implying the presence (Svendsen et al., 2004; Hughes et al., 2016) and absence (Gusev et al., 2012a) of ice sheets in the area. The absence of ice sheets is, however, inconsistent with the existence of (I) Late Pleistocene marine terraces in the Yamal and Gydan Peninsulas and (II) large unfrozen zones in the offshore extensions of major West Siberian rivers (Ob', Yenisei, Taz, and Gyda). The terraces most likely result from a 100 m sea level fall during the Zyryanian cold event (MIS-4). Their origin was possible only by subsidence and uplift due to ice loading (glaciation and low stand) and isostatic rebound (deglaciation and high stand), respectively. The unfrozen zone on the extension of the Ob', Yenisei, Taz, and Gyda river valleys is detectable by drilling and seismic surveys run by AMEGS (Kulikov and Rokos, 2017). In our opinion, it was formed in the place of a freshwater

dammed lake (Fig. 3) that existed during the MIS-2 cold event when ice obstructed the continuing river flow. Currently, the largest part of the lake contoured according to the modern bathymetry looks like a shallow-water flat, which area occupies many hundreds of thousands of square kilometers. Within it, only the paleo-valley of the Ob is expressed, it is absent from the Yenisei. The poor expression of the ancient valley network is especially clearly seen when comparing it with that in the eastern sector of the Arctic, where there were no glaciations. Paleovalleys of Khatangi-Anabar, Olenek, Lena, Indigirka, and Kolyma rivers are clearly traced in bathymetry up to the outer shelf. The existence of a dammed lake produced by an ice dam during the MIS-2 cold event is recorded in the estuaries of the West Siberian rivers, which are much longer and farther advanced than those of any other river of the Eurasian Arctic basin. The duration of its existence is explained by the length of the Ob, Taz and Pur estuaries and their flatness. Both of these indicators are close to the record, if not the record for Eurasia: the length of the Ob estuary is 800 km and the average longitudinal slope of its bottom is 1-2 cm/1 km .

Thus, the paleogeographic scenarios used by authors for reference in the modeling of this study assume the existence of ice sheets (Svendsen et al., 2004; Hughes et al., 2016). For the modeling purposes, the shelf is divided by authors into domains, subdomains, areas and subareas according to its 125 kyr history of glaciations and the respective effects on bottom sediments (Fig. 3; Table 1). The largest taxa — the domains— were distinguished by the presence / absence of glaciation and its type during MIS-2, subdomains — by the presence and impact of ice and water cover on bottom deposits in MIS-2. When specifying latitudinal zonality during periods of shelf drying, the authors followed differences in ground temperatures reflected on the Russian Geocryological Map (Yershov ed., 1991). The mean annual ground temperature is 4-6 °C lower in the NE of the region (north of Taimyr) adjacent to the Kara coast, than as for the SW (south-west of Yamal). During the periods of drainage in the periglacial part of the shelf in MIS-2, the following values for the ground temperature were taken: -19 ° C for the north-eastern area, and -15 °C for the south-western one.

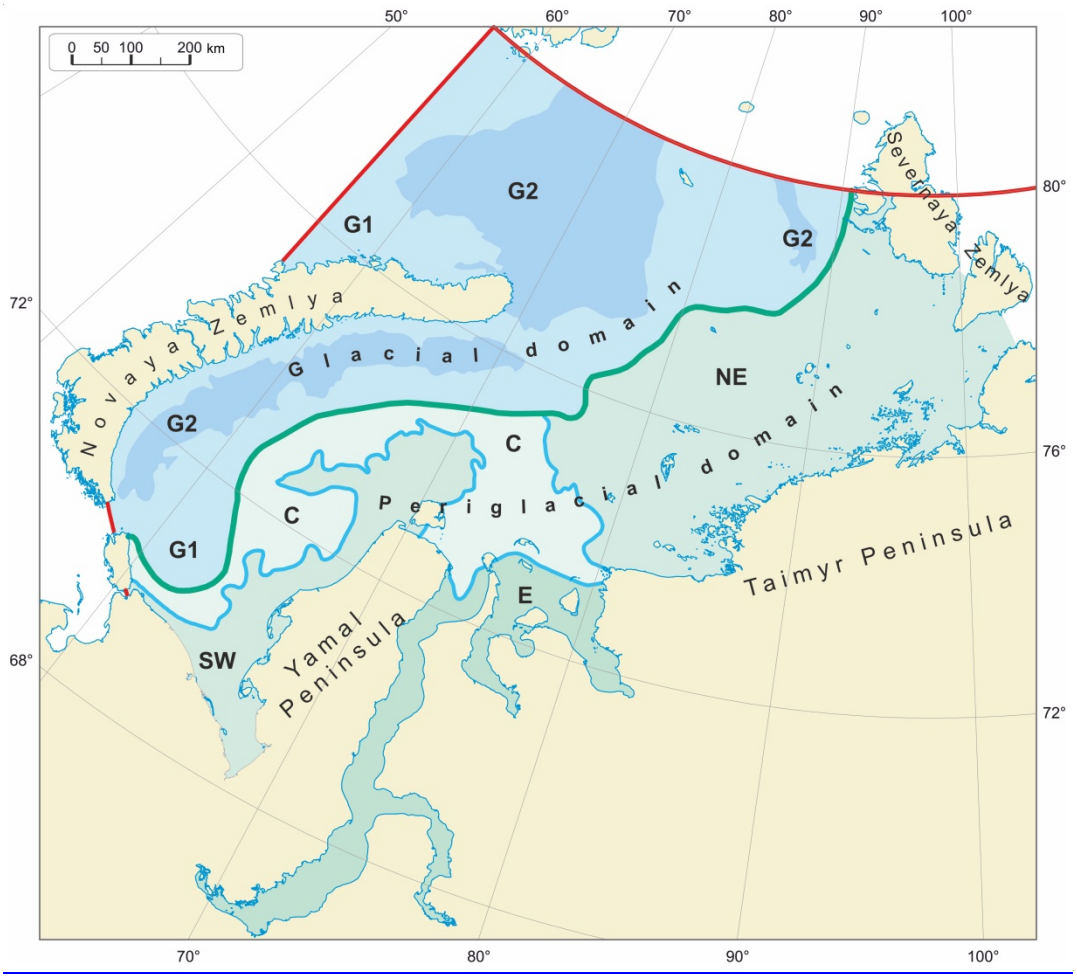

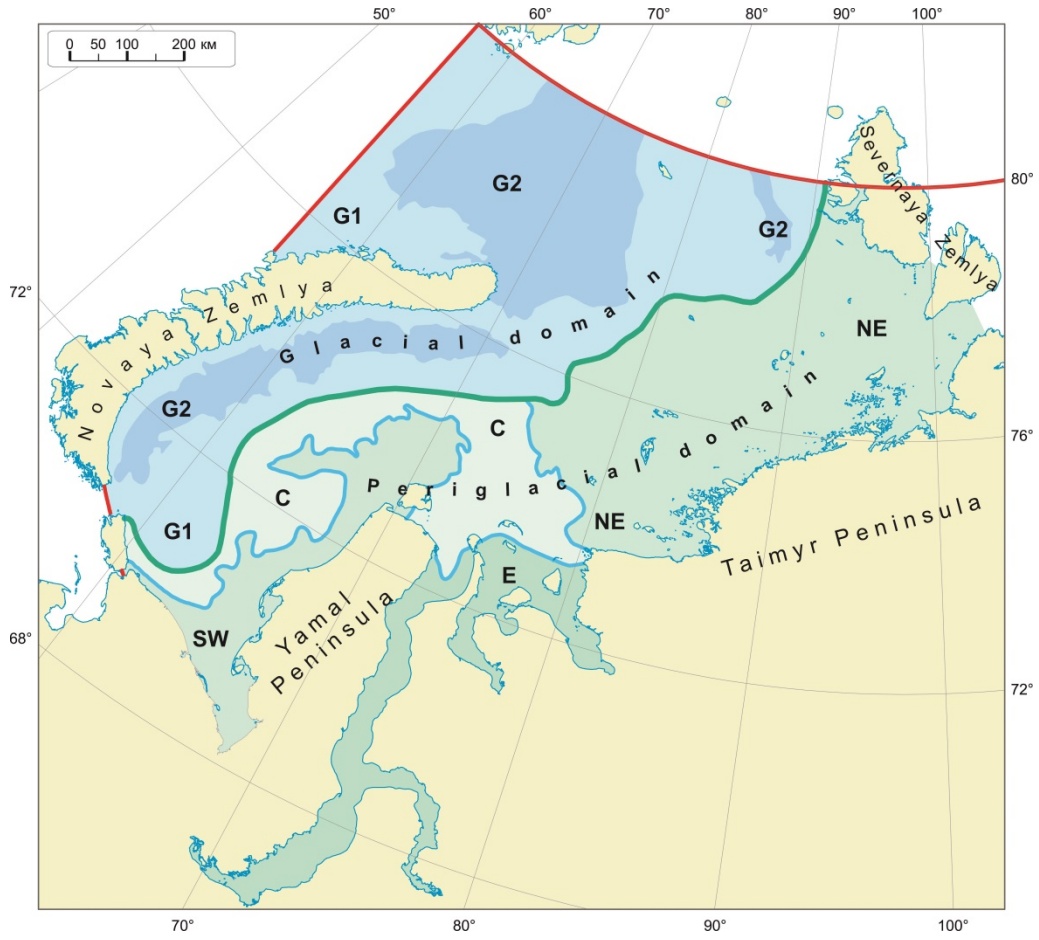

175 Fig. 3. Zoning of the Kara shelf according to its geological history for 125 kyr. Abbreviations are explained in the text and in Table 1. The red line is the research region boundary

The glacial domain includes zones where the MIS-2 ice sheet reached the sea bottom (G-1) and those of shelf ice at greater sea depths (G-2); the periglacial domain consists of subaerial and subaqual (under the ice-dammed lake) 180 subdomains, which are further divided into areas of the present sea bottom (central shelf, C) and estuaries (E) within the subaqual subdomain and southwestern (SW, 68-71 ° N) and northeastern (NE, 72-77 ° N) shelf parts within the subaerial subdomain (Fig. 3; Table 1). The SW and NE areas had different landscapes during MIS-2 and, correspondingly, differed in ground temperature and freezingdepth. The areas C and E were flooded by cold (<0°C) sea water and warmer (>0°C) river water, respectively, in the Holocene

185

Table 1. Zoning of the Kara shelf (Late Pleistocene-Holocene history, past 125 kyr, events MIS-2 – MIS-1)

Domains	Subdomains	Areas (landscapes)		Subareas
Periglacial domain	Subaerial	Southwestern shelf	**SW**	Sea depths 0-120 m (contour intervals of average depths at 5, 20, 50, 80 and 100 m)
		Northeastern shelf	**NE**	
	Subaqual (under ice-dammed lake) for 25-15 kyr	Central shelf	**C**	Sea depths 0-80 m
		Estuaries	**E**	
Glacial domain, ice reaching sea bottom	Subaqual (for 7-10 kyr)	**G-1**		Sea depths 0-200 m
Glacial domain, shelf ice, MIS-2	Subglacial-subaqual	**G-2**		Sea depths 200-800 m

190

Finally, the periglacial areas were divided into subareas according to sea depths which controlled the duration of permafrost formation during regressions and degradation during transgressions: 0-10, 10-35, 35-65, 65- 90 and 90-140 m sea depth intervals with average values of 5, 20, 50, 80, and 120 m, respectively.

The subdomains of ice contacting(G-1) or not (G-2) the sea bottom were revealed from seismoacoustic data, with reference to the 1:2 500 000 Map of Quaternary deposits (2010): acoustically transparent deposits (below isobaths 200 m) were considered as glacial-marine. Glaciers in these places were treated as shelf ice. The zones G-1 and G-2 are only shown in Fig. 3 and Table 1 and were not divided further. The modeling we carried out for the G-1 area showed that, to date, the permafrost formed in the MIS-2 have not survived.

The present permafrost in the region formed under the effect of climate-driven eustatic sea level change. The sea level curve for the 125-15 kyr period was plotted using the eustatic curves of Lambeck and Chappell (2001) and Siddal et al. (2003, 2006). These curves were adapted to the regional specificity (Trofimov et al., 1975; Streletskaya et al., 2009; Shishkin, M.A. et al., 2015), with regard to Late Pleistocene marine terraces in Yamal interpreted in the context of ice waxing and waning. Special focus by authors was in the recreating on the Late Pleistocene-Holocene transgression (Fig. 4Aa,Bb). The Figure 4Cc shows the scenario on fluctuations of the sea level during the modeling period of 125-15 kyr..

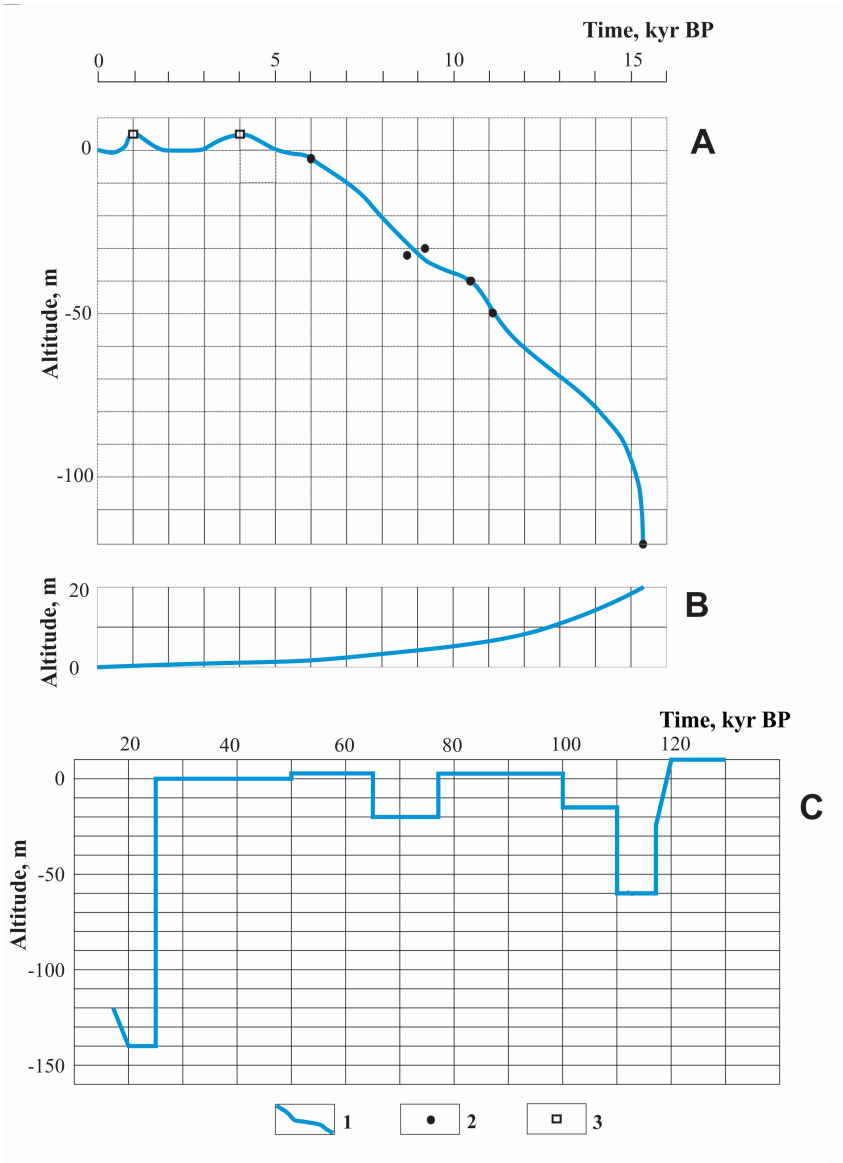

Fig. 4. Scenarios of sea level fluctuations:
for the 15-0 kyr .: A -periglacial domain, B- glacial domain; for the 125-150 kyr: C - periglacial domain.

1 - sea level curve; 2 - dated bottom sediment cores from Ob' Gulf, Yenisei Gulf, and adjacent offshore (Stein, et al., 2009) and Vilkitsky Strait (Levitan.et al., 2007) sites; 3 - onshore data (Romanenko, 2012);

In the method of constructing a scenario of sea level fluctuations for the Kara shelf, the accounting for glacio-isostatic movements, resulting in the formation of marine terraces (Gutenberg, 1941; Flint, 1957; Bylinsky, 1996), plays a large role. The reason for their formation is the sea flooding of the glacier bed, with a lag reacting to the removal of the glacial load. Therefore, during the reconstructions, post-glacial sea level fluctuations are divided into two categories. In non-glacial areas, sea level rises in relation to the nearest coast, in glacial areas it drops (Lambeck, Chappell, 2001).

In accordance with the above, the scenario is presented in the form of curves for the periglacial (with respect to the continent, Fig. 4A) and glacial (with respect to Novaya Zemlya, Fig. 4B) domains. The periglacial curve was obtained with reference to published evidence on the Laptev Sea (Bauch et al., 2001), and the glacial one was calculated according to data on isostatic subsidence and uplift during glaciation and deglaciation, respectively (Ushakov and Krass, 1972; Nikonov, 1977; Bylinsky, 1996). Figure 4 shows that the calculations for the glacial domain were made taking into account (I) the thickness of the MIS-2 ice sheet (rising 500 m above the m sea bottom subsidence under the ice load; the fall reached 140 m, or 20 m below the global average regression limit (Lambeck and Chappell, 2001).

In postglacial times, the sea level rose during transgression in the periglacial domain but fell in the glacial one as a result of Novaya Zemlya uplift. Thus, the glacial domain was exposed to weaker cooling during the glacial period and became flooded and exposed to permafrost degradation right after ice melting. Unlike this, flooding in the periglacial domain was accompanied by permafrost degradation for as long as 1500 years.

The construction of scenarios of groundtemperature dynamics by the authors during the estimated time is the final part of the paleogeographic materials for the conduction of the numerical modeling. The ground temperatures were reconstructed in several 1D solutions, with reference to paleo-water chemistry (Fotiev, 1999; Volkov, 2006) and oxygen isotope composition of ice wedges (IW, $\delta^{18}O_{IW}$) (Vasil`chuk, 1992), as well as to reconstructed summer air temperatures. The $\delta^{18}O_{IW}$ data were corrected according to the results of Golubev et al. (2001).

We present the paleogeographic scenario as a series of paleotemperature curves adapted to the modeling purposes (Figs. 5, 6~~7~~). In the following, the plots of mean annual ground temperatures of over the past 125 kyr depending on paleogeographic events (shelf drainage, flooding, glaciation, etc.), and in connection with the existence of latitudinal zoning and meridional sectorality are presented When specifying latitudinal zonality during periods of shelf drying, the authors followed differences in ground temperatures reflected on the Russian Geocryological Map (Yershov ed., 1991). The mean annual ground temperature is 4-6 °C lower in the NE of the region (north of Taimyr) adjacent to the Kara coast, than as for the SW (south-west of Yamal). When zoning the shelf (Table 1, Fig. 3), the southwest (68-71 ° N) and north-eastern (72-77 ° N) areas were distinguished. During the periods of drainage in the periglacial part of the shelf in MIS-2, the following values for the ground temperature were taken: -19 ° C for the north-eastern area, and -15 °C for the south-western one .~~Altogether thirty such curves have been obtained, each based on four lithological patterns and two heat flux values.~~

The initial conditions are those given for the interglacial MIS-5e . There was a warm-water sea basin on the Kara shelf and adjacent lowlands from 140 to 117 kyr (Fig. 5, 6) (Astakhov and Nazarov, 2010; Nazarov, 2011; Gusev et al., 2016a). Preliminary modeling for the interval MIS-6 - MIS-5e (200-117 kyr BP) showed that previously formed permafrost completely thawed under the sea during MIS-5e, which had existed for more than 20 kyr.The sequence of paleogeographic events in the form of a series of cartographic schemes is shown in Fig. 7.

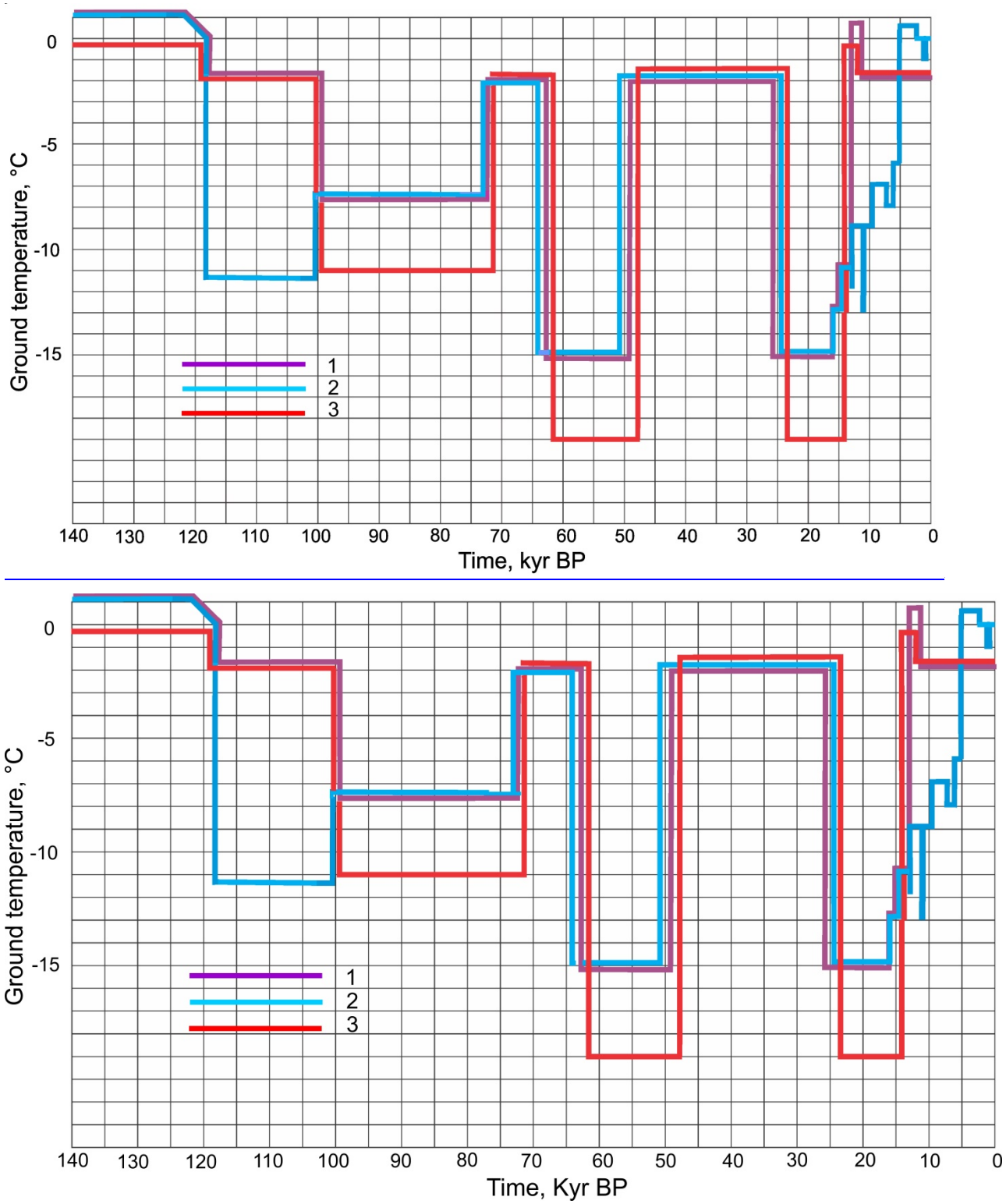

Fig. 5. Paleo-temperature curves for the periglacial subaerial part of the shelf:
1 = southwestern shelf part (SW), 80 m isobath; 2 = southwestern shelf part (SW), 5 m isobath;
3 = northeastern shelf part (NE), 120 m isobath.

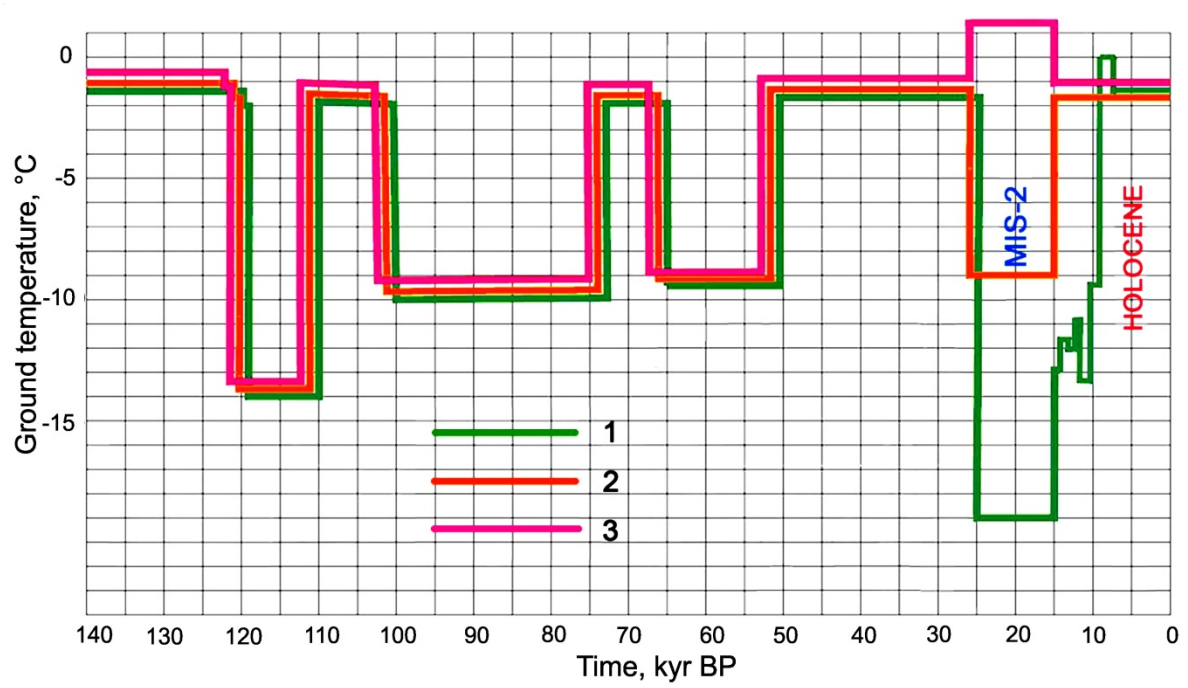

Fig. 67. ~~Paleogeographic scenario~~ Paleo-temperature curves for 50 m isobath :~~for MIS-2 which controlled the present distribution of frozen and cooled ground. Adapted for modeling purposes. A fragment.~~

1 = periglacial subaerial northeastern shelf part (**NE**); 2 = ice that reached the bottom for 7-10 kyr, **G-1**); 3 = subaqual (beneath damlake) central shelf part, **C**;

MIS-5e (140-117 kyr BP)

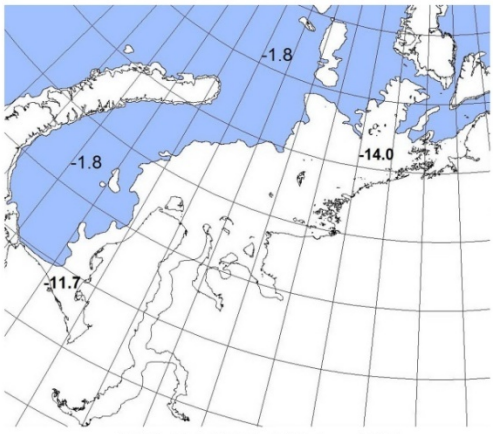

MIS-5d (117-110 kyr BP)

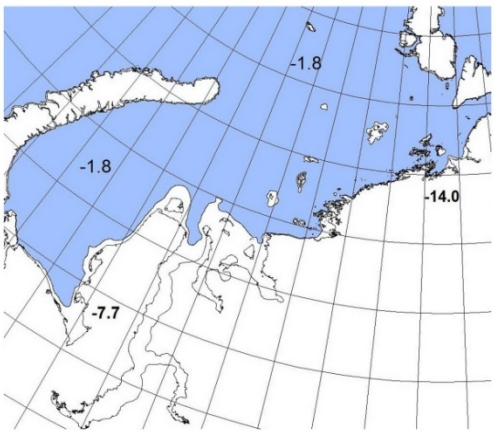

MIS-5c (110-100 kyr BP)

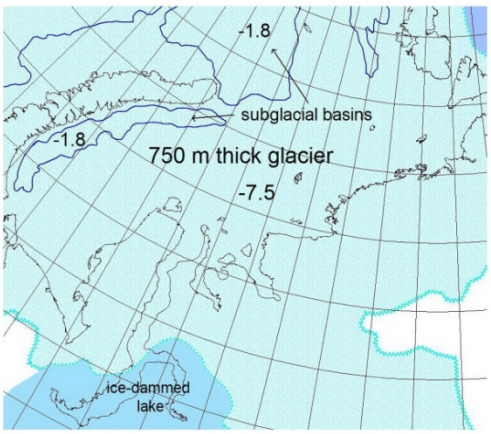

MIS-5b (100-77 kyr BP)

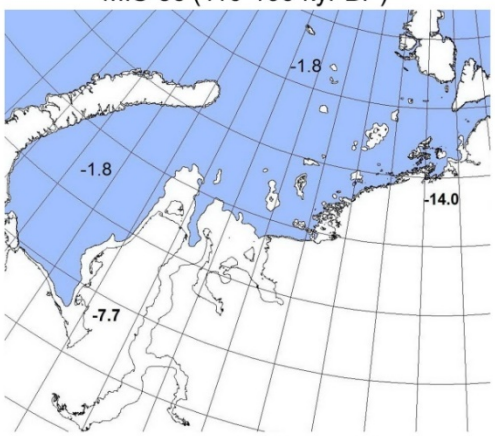

MIS-5a (77-65 kyr BP)

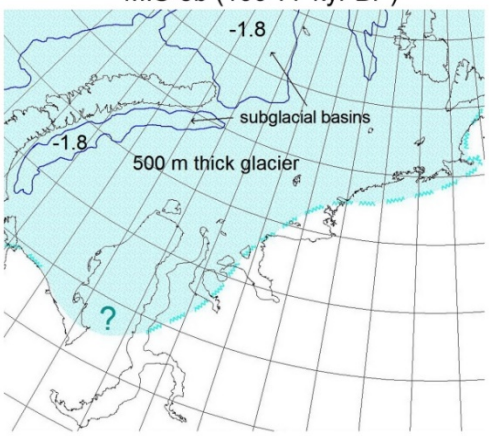

MIS-4 (65-50 kyr BP)

MIS-3 (50-25 kyr BP)

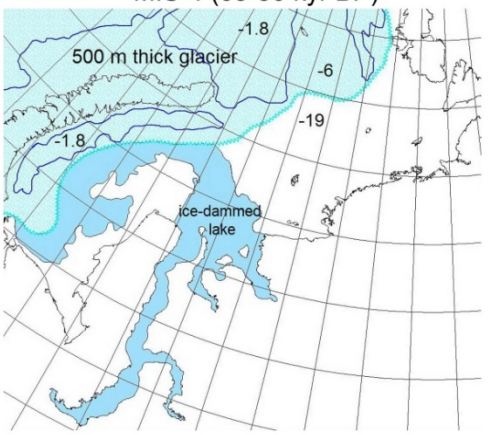

MIS-2 (25-15 kyr BP)

Fig. 7. The series of cartographic schemes illustrating the change in surface conditions in the Kara Sea shelf for the following moments : MIS 5e (140-117 kyr); MIS 5d (117-110 kyr); MIS 5c (110-100 kyr); MIS 5b (100-77 kyr); 5a (77-65 kyr); MIS -4 (65-50 kyr); MIS -3 (50-25 kyr); MIS -2 (25-15 kyr).

Altogether thirty curves have been obtained, each based on four lithological patterns and two heat flux values.

~~During transgressions in the Holocene~~ An important role in the formation of the current permafrost is the last (Holocene) transgression of the sea. Therefore, it was set that~~,~~ that each shelf part stayed for 400-2000 years in the coastal zone where bottom sediments were flooded with saline and warm near-bottom water. It is known that at sea depths from 2 to 7 m in the 1970s (Zhigarev, 1981), up to 10 m in the 2000s. (Dmitrenko) the mean annual temperature of bottom waters in the Laptev Sea stays positive and bottom sediments thaw from above. For the Kara Sea, there are no such data on isobath intervals, but it is known that temperatures are generally lower. Therefore, we assumed that the interval of isobaths with such water temperatures was limited to 5-6 m. Episodes with such water temperatures occurred on the shelf during the postglacial transgression even in its initial periods, since the July temperature is reconstructed for pre-Holocene warming (allered) exceeding 2 ° C the temperature of the 1980s. (Velichko et al., 2000). Therefore, we constructed scenarios for these episodes. To determine their duration, dated data on the absolute altitudes of the sea level during the transgression of the Laptev Sea were used (Bauch et al., 2001). The transgression rate was not the same. The shortest episodes (400 and 375 years) of positive temperatures are determined for periods 15-11 and 10-9 ka respectively. The longest intervals were 11–10, 9–5, and 5–0 Ka with 1000, 750 and >5000 years according to simple calculations. Special mathematical modeling for desalinated coastal zones was not performed due to the relatively small area of their distribution and the specific nature of salinity distribution over the water column. Desalination of waters was taken into account directly when constructing a geocryological map.

The scenarios record alternated cold and warm events accompanied, respectively, by regressions and transgressions (Figs. 5, 6, 7), which created conditions for permafrost growth and degradation. At glaciation peaks, the present sea bottom in the periglacial shelf part was above the shores which subsided under the ice load. This led to the formation of marine terraces, i.e., the sea level fall during cold events (MIS-5b, MIS-4) was smaller than the global average.

The available data, though far incomplete, show that the sea level between 50 and 25 kyr BP(almost all MIS-3 through) was the same as at present (Fig. ~~6~~8), in our opinion it is also due to post-Zyryanian uplift (isostatic rebound). On the other hand, the current state of permafrost has been controlled by the ground temperature in the periglacial shelf part and by the presence of an ice-dammed freshwater basin (Fig. ~~7~~6). In the Holocene, the effect of >0 °C bottom water in the near-shore zone during warm climate events was critical for permafrost degradation from above (Figs. 5~~.~~,6 ~~7~~). The MIS-2 ground temperature in the glacial shelf part was warmer (Fig. ~~7~~6, the curve 2) due to thermal insulation by ice.

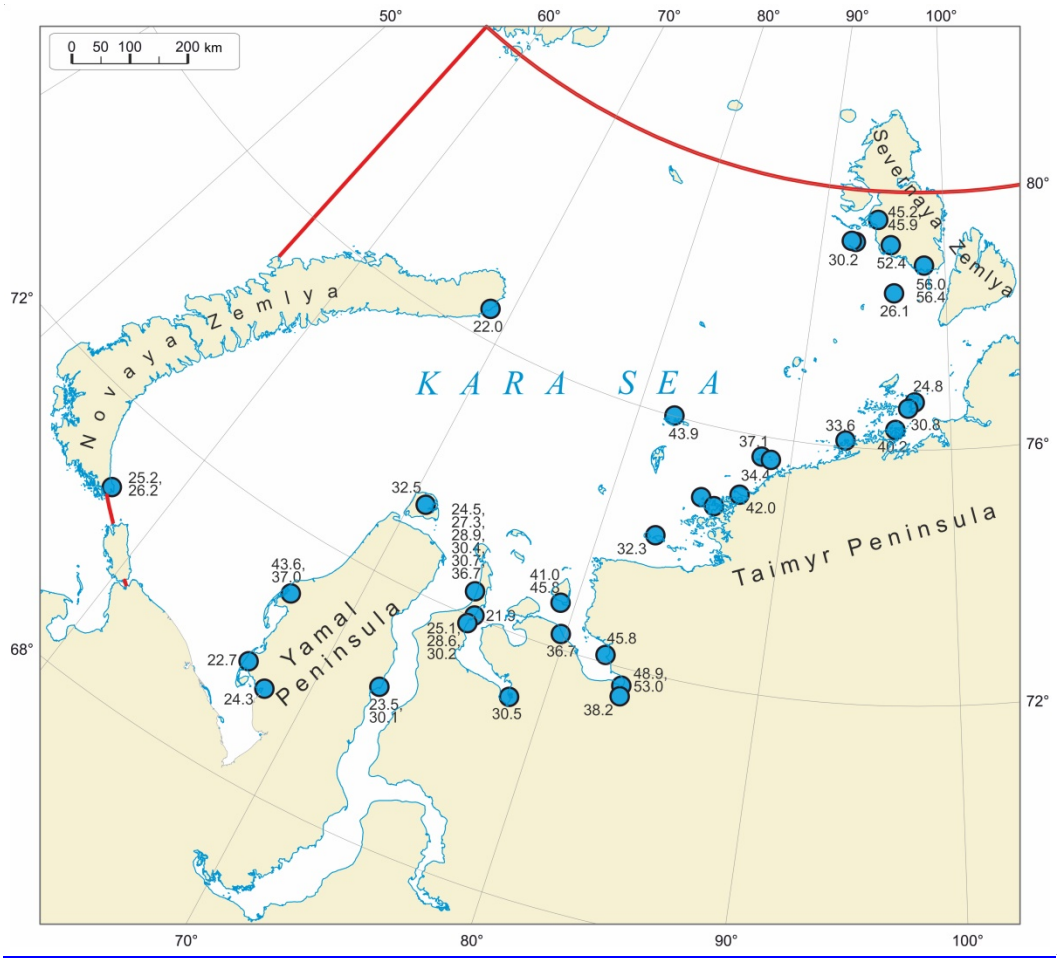
0 50 100 200 km
50°
60°
70°
80°
90°
100°
72°
68°
76°
80°
Severnaya Zemlya
Novaya Zemlya
KARA SEA
Taimyr Peninsula
Yamal Peninsula
45.2
45.9
30.2
52.4
56.0
56.4
26.1
22.0
24.8
30.8
33.6
40.2
43.9
37.1
34.4
42.0
32.3
25.2
26.2
32.5
24.5
27.3
28.9
30.4
30.7
36.7
43.6
37.0
41.0
45.8
21.9
25.1
28.6
30.2
36.7
45.8
48.9
53.0
38.2
22.7
24.3
23.5
30.1
30.5

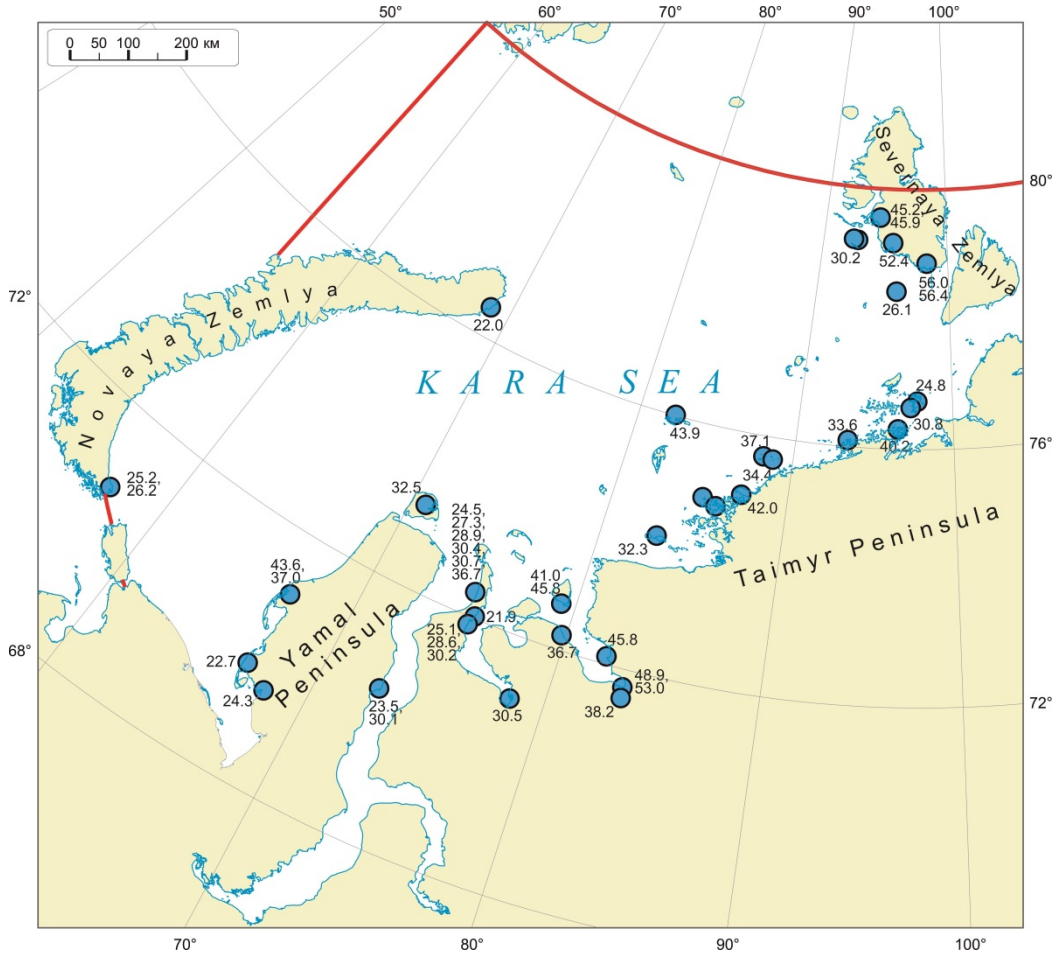
0 50 100 200 км
50°
60°
70°
80°
90°
100°
72°
68°
76°
80°
Severnaya Zemlya
Novaya Zemlya
KARA SEA
Taimyr Peninsula
Yamal Peninsula
45.2
45.9
30.2
52.4
56.0
56.4
26.1
22.0
24.8
30.8
33.6
40.2
43.9
37.1
34.4
42.0
32.3
25.2
26.2
32.5
24.5
27.3
28.9
30.4
30.7
36.7
43.6
37.0
41.0
45.8
21.9
25.1
28.6
30.2
36.7
45.8
48.9
53.0
38.2
22.7
24.3
23.5
30.1
30.5

Fig. 8~~6~~. Location of onshore and offshore sections (points) with marine sediments (^{14}C - figures, thousand years ago) of MIS-3 in the Kara Sea shelf, after Gusev et al. (2011; 2012a, b; 2013a, b; 2016 a, b); Baranskaya et al. (2016); Vasil`chuk et al. (1984); Molodkov et al. (1987); Bolshiyanov et al. (2009). The red line is the research region boundary

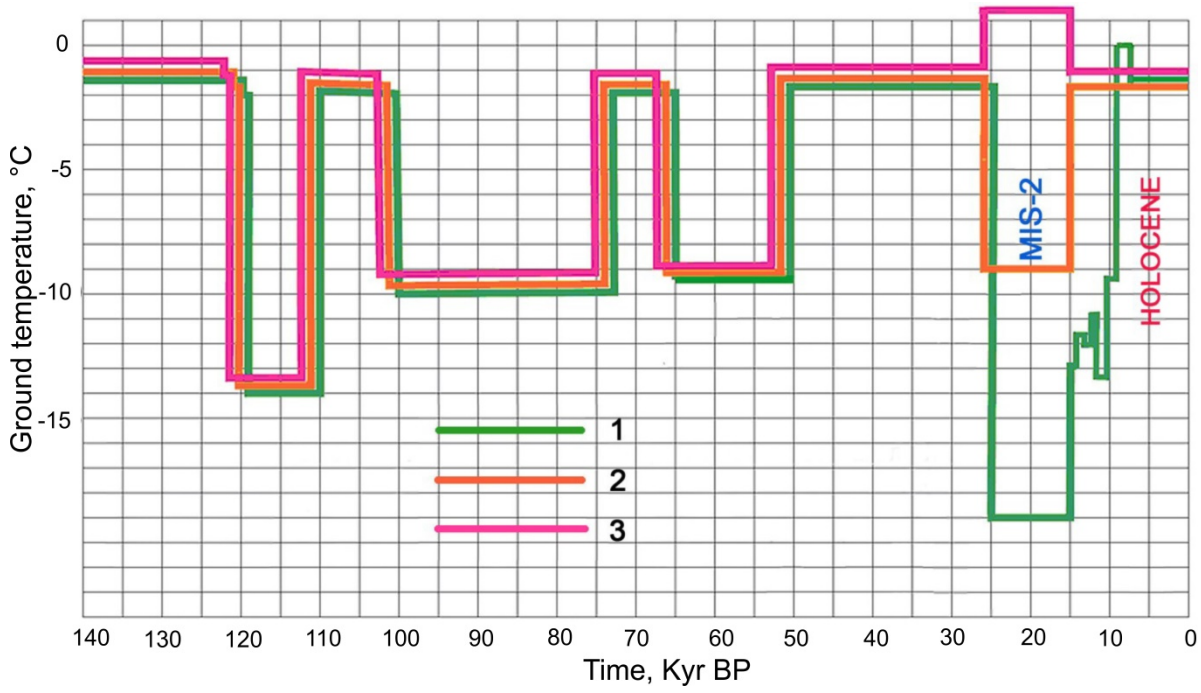

~~The series of cartographic schemes illustrating , the change in surface conditions for the 125 kyr history of the Kara sea shelf is presented in the Fig. 8.~~

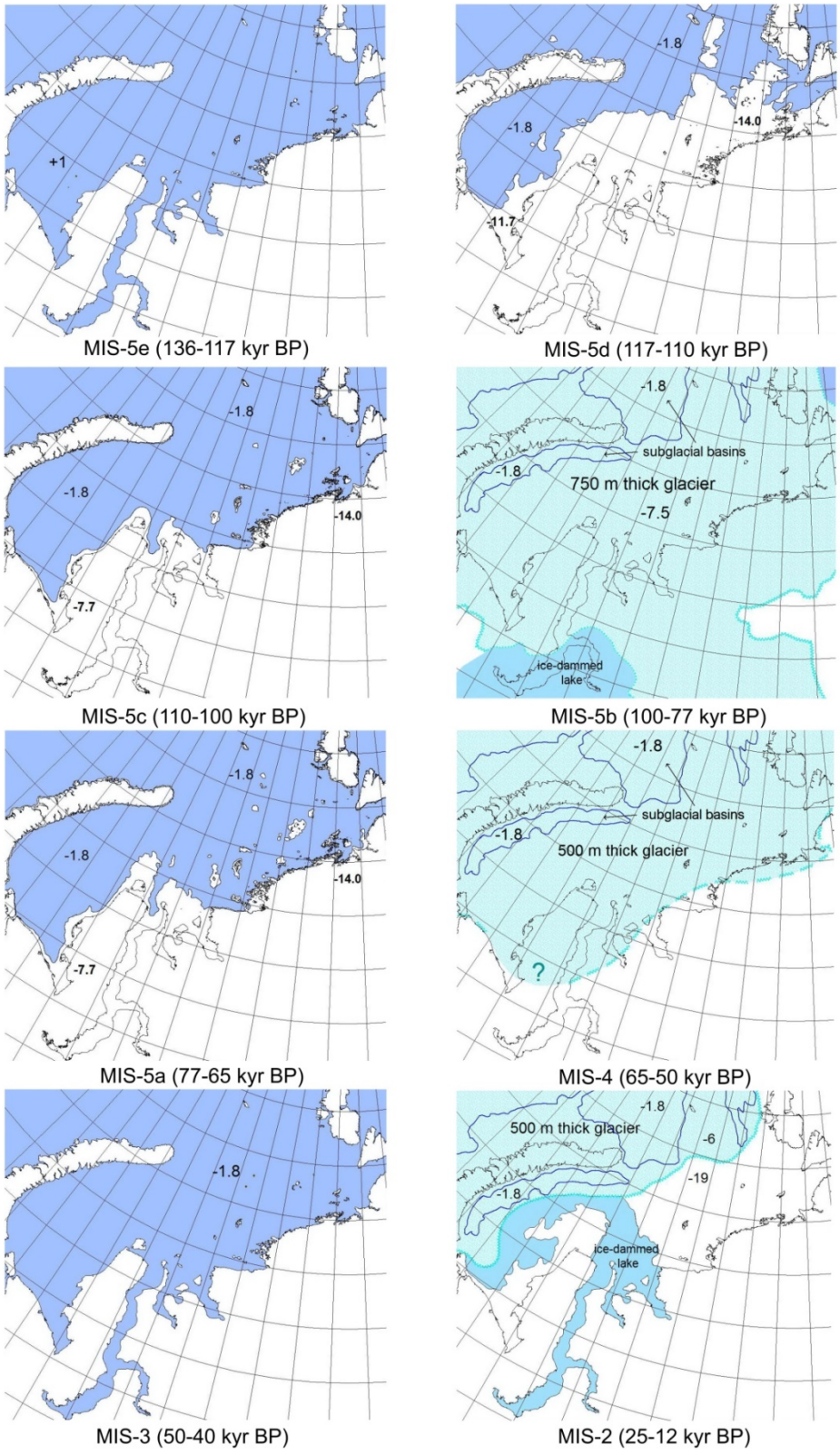

305

~~Fig. 8. The series of cartographic schemes illustrating , the change in surface conditions in the Kara Sea shelf for the following moments : MIS 5e (130-120 kyr, MIS 5d (117-110 kyr) MIS 5c (110-105 kyr); MIS 5b (100-75 kyr); 5a (75-65 kyr); MIS -4 (kyr); MIS -3 (50-25kyr); MIS -2 (25-15 kyr)~~

310 **4. Simulation results and regional interpretation**

The simulation results show that the distribution of depositsthat differ in their state (thawed, cooled, frozen) are associated with the paleogeographic events of the Late Pleistocene-Holocene. In the distribution of permafrost, a particularly close relationship occurs with glaciation in the MIS-2, the postglacial epoch and the Holocene optimum.

4.1. Distribution of frozen, cooed, and thawed deposits

Here we consider the permafrost table (frozen permafrost) corresponds to the -1.8° C isotherm, Therefore further in the text we mean frozen permafrost when talking about «permafrost» and the cryotic unfrozen deposits are «cooled» deposits (marine cryopeg). Permafrost occurs within the areas that were free from MIS-2 ice sheets (SW, NE, C and partly E in Figs. 3,9; ~~Figs. 8, 9, 10~~). The present areas of cooled ground were covered with ice that reached the sea bottom during MIS-2 (Fig. 3). Thawed deposits occupy the areas which were open to the inflow of >0 °C Atlantic waters (Levitan et al., 2009) in early postgalacial time (16-15 kyrBP): a part of the G-2 zone (Fig. 3) and a large part of estuaries (E in Fig. 3), except for their northern ends.

Frozen ground is restricted to the periglacial domain. The boundary between the periglacial and glacial domains and, correspondingly, between the frozen, cooled and thawed deposits is delineated by the limits of MIS-2 ice that reached the sea bottom and remained in contact with it for 7-10 thousands of years (Fig. 3), and by the 120 m isobath in the northeastern shelf part, within Severnaya Zemlya and the Cheluskin Peninsula (Figs. 3, 9~~8~~).

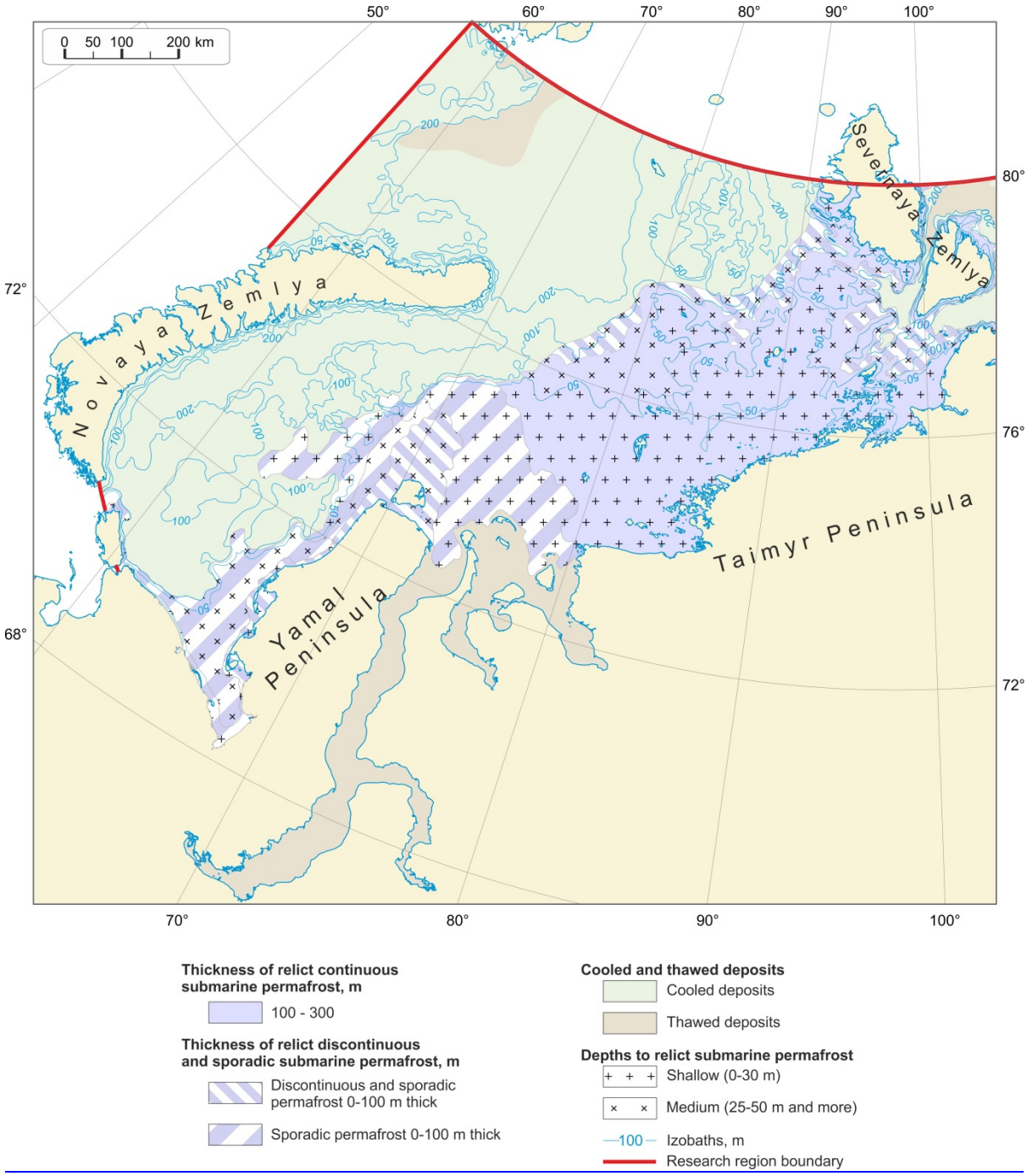

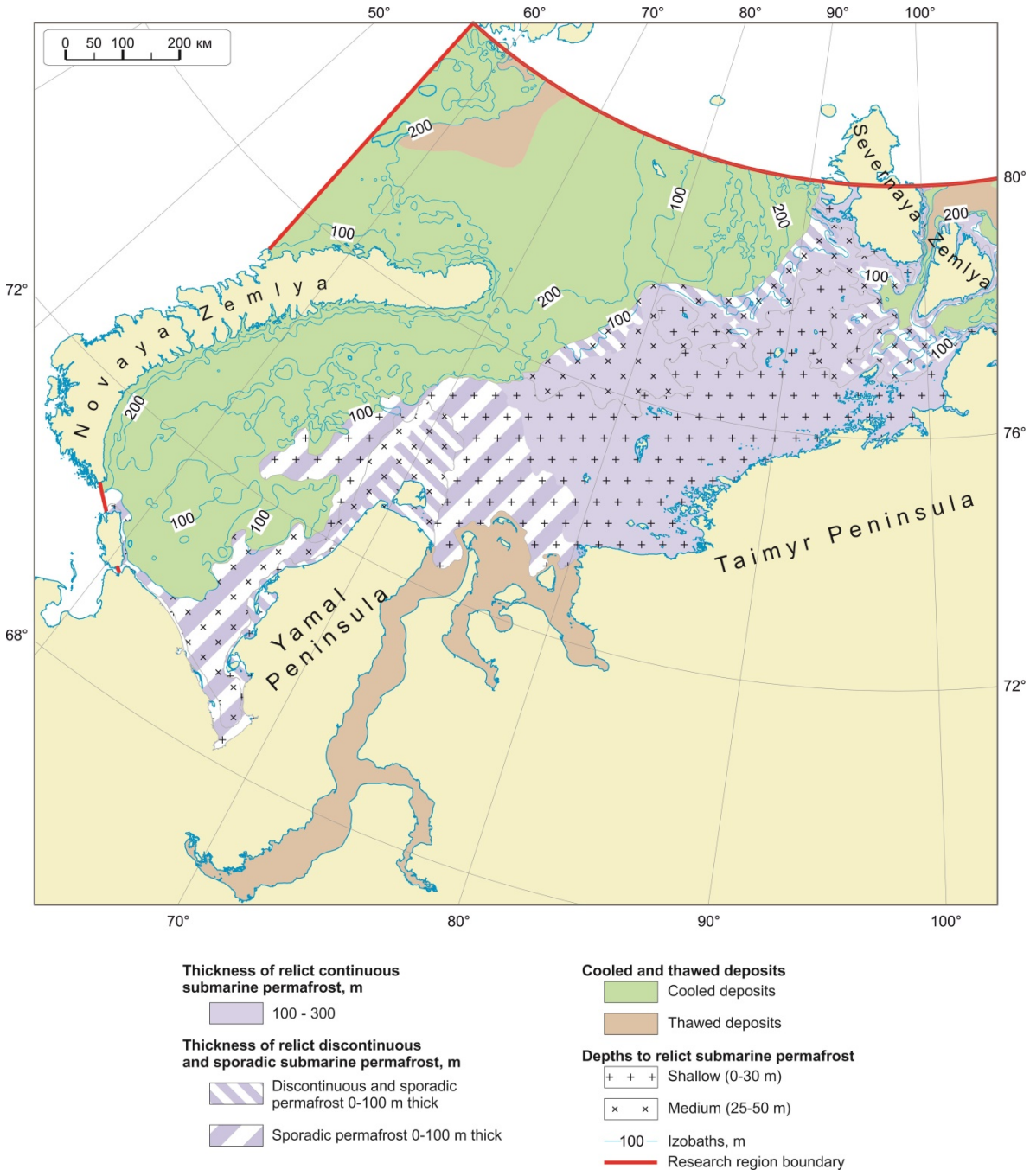

Fig. 9. Fragment of the geocryologic map of the Kara Sea and its legend.

4.2. Distribution of permafrost, its thickness and depth to the permafrost table

Permafrost becomes more extensive, shallower and thicker from southwest to northeast and from deep offshore toward near-shore shallow waters. This pattern has several controls (Supplementary Figure 1):

(1) latitudinal climatic zonation and division into sectors;

(2) sea depths that affect the duration of shelf drying and flooding (permafrost formation and degradation, respectively);

(3) ice-dammed freshwater basin in MIS-2;

(4) geothermal heat flux;

(5) lithology and properties of deposits;

(6) sea water and seasonal ice cover (salinity and freezing-thawing temperatures of deposits);

(7) thermal effect of river waters;

(8) Holocene climate optimum.

The southwestern part of the Kara Sea experienced an impact of warm water inputs (Pogodina, 2009) in the middle Holocene (the Holocene optimum), judging by the distribution of thermophile foraminifera communities with predominant Arctic-boreal species found currently in the Pechora Sea. Therefore, the >0 °C bottom water temperatures common to the present-day Pechora Sea may have existed 7-5 kyr in the southwestern Kara shelf and provided thawing of permafrost from above.

The distribution of permafrost also depends on deep heat flux which may reach 50-60 mW/m^2 over the greatest part of the Kara shelf (Khutorskoi et al., 2013). Temperature logs from deep boreholes in the shelf and coastal gas reservoirs of Yamal give heat flux values of 73-76 mW/m^2. Other controls include lithology, water contents, physical properties, and salinity (freezing-thawing temperatures) of deposits .

Tables 2 and 3 lists the most common depths to the permafrost table determined in previous studies and according to our own calculations. They may vary significantly, even within marine geosystems of the same type: according to drilling results, they are 56 m in the near-shore zone at the Kharasavei Cape and as shallow as 5 m in the Sharapov Shar Gulf 50-60 km in the south. The prospective values are 30-40 m below the sea bottom under the Yamal shores and close to the water table under the retreating coast (Baulin et al., 2005). The permafrost thickness was estimated as the difference between the depths to permafrost table and base

4.2.1. Southwestern periglacial shelf

The southwestern part of the Kara shelf (SW in Fig. 3) is occupied by discontinuous and sporadic permafrost (Fig. 8), as inferred from modeling with reference to field data (Dlugach and Antonenko, 1996; Melnikov and Spesivtsev, 1995; Baulin, 2001; Bondarev et al., 2001; Rokos et al., 2001, 2007, 2009; Baulin et al., 2005; Neizvestnov et al., 2005; Kulikov and Rokos, 2017). According to the modeling results, permafrost can exist in sand at a heat flux of 50 mW/m^2 but is absent in all other lithologies at 75 mW/m^2 (Table 2).

Table 2. Modeling results for depths to permafrost top and base and permafrost thickness, uniform lithology, SW area

Sea depth, m	Lithology	Geothermal heat flux, mW/m^2					
		50			75		
		Depth to base, m	Depth to top, m	Thickness, m	Depth to base, m	Depth to top, m	Thickness*, m
5	sand	190	50	140	175	55	120
	clay silt	110	45	65	0		
	bedrock	150	45	105	0		
20	sand	180	50	130	140	60	80
	clay silt	75	40	35	0		
50	sand	175	50	125	130	60	70
	clay silt	0			0		
	bedrock	120	60	60	0		
80	sand	165	65	100	82	55	27
120	sand	0			0		
	clay silt	0			0		
	bedrock	0			0		

*the quoted permafrost thicknesses in all tables here and below are current residual values.

Table 3. Modeling results for depths to permafrost top and base and permafrost thickness, alternated sand and clay silt (clay), SW area

Sea depth, m	Alternating layers, 0.5 and 0.3 volumetric fraction of sand (n_n)	Geothermal heat flux, mW/m^2					
		50			75		
		Depth to base, m	Depth to top, m	Thickness, m	Depth to base, m	Depth to top, m	Thickness, m
5	n_n=0.5	133	40	93	0		
	n_n=0.3	117	40	77	0		
50	n_n=0.5	132	50	82	0		
	n_n=0.3	124	55	69	0		
120	n_n=0.5	0			0		
	n_n=0.3	0			0		

375

Table 4. Modeling results for depths to permafrost top and base and permafrost thickness, 50 m of alternated sand and clay silt (clay) lying over bedrock, SW area

Sea depth, m	Alternating layers, 0.5 and 0.3 volumetric fraction of sand (n_n)	Geothermal heat flux, mW/m^2					
		50			75		
		Depth to base, m	Depth to top, m	Thickness, m	Depth to base, m	Depth to top, m	Thickness, m
5	n_n=0.5	129	40	89	0		
	n_n=0.3	115	40	75	0		
50	n_n=0.5	130	55	75	0		
	n_n=0.3	127	57	70	0		
120	n_n=0.5	0			0		
	n_n=0.3	0			0		

The quantitative modeling results show (Table 2) that the permafrost state depends on lithology if it is uniform. However, the real shelf sections (e.g., in boreholes of the Leningradskaya and Rusanovskaya fields) consist of different alternating lithologies. Therefore, data listed in Table 2 are applicable uniquely as a check for the role of lithology and properties in the formation, distribution and thickness of permafrost, and in depths to its top and base, which were estimated for layered sections.

Along the west coast of the Yamal Peninsula (area of the Kharasavei-Sea field), where the modern frozen deposits form the upper part of the section, and the relict ones are underlain, permafrost in the Kharasavei shelf gas and condensate deposit forms three elongate zones: ~0.5 km wide zone of continuous permafrost near the shore (0-2 m sea depth); discontinuous permafrost, 1-3 km wide, sea depths to 5-7 m (Baulin, 2001; Baulin et al., 2005); and sporadic permafrost, which may spread to sea depths of 80 m (our estimate), or 100 m (Kulikov and Rokos, 2017) to 105 m (Vasiliev et al., 2018).

The depths to the permafrost table are variable, especially near the shore, as a result of coastal advance and retreat. Permafrost currently exists in zones of coast aggradation, while permafrost beneath retreating coasts is the shallowest at the shoreline and becomes deeper seaward. Specifically, permafrost was stripped at a depth of 0.5 m below the sea bottom at the geocryological site Marre-Sale, in borehole 16-14 drilled for temperature monitoring 0.5 km far from a retreating coast (Dubrovin et al., 2015) but is deeper (3.5 m) in another monitoring borehole 15-14 located 0.9 km far from the shore, where a 0°C mean annual ground temperature was recorded at 3 m subbottom depth. On the other hand, the permafrost table beneath stable coast may be as deep as 30-50 m (Baulin et al., 2005). Similar depth variations occurred also during the Holocene transgression, i.e., this is a typical feature of local permafrost. However, generally the depths to permafrost increase offshore and depend on its composition and ice content, as well as on the time when it submerged.

Within the sea depths from 2 to 5-7 m, the depth to permafrost varies from 5 to 30-40 m. Similar values were inferred by modeling for the most realistic sections of interbedded sand and clay (40 m at a heat flux of 50 mW/m^2). The calculated most probable permafrost thickness for these lithologies is 75-90 m at 50 mW/m^2. It agrees with 60-80 m reported by Badu (2014) as well as with the estimates 90 m and 70 m by Vasiliev et al. (2018) for the sea depths about 10 m and 35 m, respectively. Permafrost in terrace I of Yamal, which formed from MIS-2 through the Holocene and was not exposed to prolonged subsea degradation, is as thick as 185 m (Trofimov et al., 1975; Yershov, 1989).

According to calculations, on isobaths exceeding 7-10 m, the subsea permafrost table is as deep as 50-80 m (Table 3), which agrees with estimates based on field data (Melnikov and Spesivtsev, 1995). It is most likely beyond the reach of engineering geological drilling (Baulin et al., 2005).

Permafrost is discontinuous to sporadic closer to the shore and sporadic at greater sea depths, with the boundary at the 10 m isobath. The depths to permafrost table are 0-30 in two first zones and 20-50 m in the offshore zone. The permafrost thickness is from 0 to 100 m (Fig. 9).

Similar distribution and parameters of permafrost are common to other parts of the southwestern periglacial shelf, but they vary slightly as a function of zonal features. Farther in the north, the boundary between discontinuous and sporadic permafrost follows the 20 m isobath. The depths to the permafrost table are 30 to 70 m at sea depths from 0 to 20 m according to field data, and 40 to 70 m according to calculations; the calculated permafrost thickness is mainly <100 m (the estimates in Table 2 are for reference sections and those in Tables 3-4 are real data). In real sections within 20-80 m sea depths, permafrost lies at a depth of 50-55 m and is 70-90 m thick (Tables 3-4).

The permafrost changes form discontinuous to sporadic below the 5 m sea depth south of the Kharasavei deposit and is only sporadic still farther to the south (end of the Baidaratskaya Guba Bay).

4.2.2. Northeastern periglacial shelf

There is no drilling data for this shelf part (NE in Fig. 3; Fig. 8). According to logs from a test well in Sverdrup Island, heat flux, varies from 25 to 60 mW/m^2 as a function of lithology and thermal properties of rocks and sediments at different core depths (Khutorskoi et al., 2013). Modeling results for a heat flux of 50 mW/m^2 predict that the permafrost is continuous at sea depths within 0-80 m and discontinuous to sporadic from 80 to 120 m (Tables 5-7). Cooled rocks may exist at these sea depths mainly in clay sediments, at different heat flux values, though permafrost is predominant (Tables 5-7).

Table 5. Modeling results for depths to permafrost top and base and permafrost thickness, uniform lithology, NE area

Sea depth, m	Lithology	Geothermal heat flux, mW/m^2					
		50			75		
		Depth to base, m	Depth to top, m	Thickness, m	Depth to base, m	Depth to top, m	Thickness, m
5	sand	270	25	245	175	25	150
	clay silt	130	20	110	0		
	bedrock	190	28	162	0		
20	sand	260	30	230	160	32	128
50	sand	250	35	215	150	35	115
	clay silt	120	35	85	0		
	bedrock	170	40	130	0		
80	sand	230	40	190	105	40	62
120	sand	212	50	162	85	50	35
	clay silt	0			0		
	bedrock	90	50	40	0		

Table 6. Modeling results for depths to permafrost top and base and permafrost thickness, alternated sand and clay silt (clay), NE area

Sea depth, m	Alternating layers, 0.5 and 0.3 volumetric fraction of sand (n_n)	Geothermal heat flux, mW/m^2					
		50			75		
		Depth to base, m	Depth to top, m	Thickness, m	Depth to base, m	Depth to top, m	Thickness, m
5	n_n=0.5	221	20	201	107	20	87
	n_n=0.3	190	20	170	75	20	55
50	n_n=0.5	206	35	171	91	38	53
	n_n=0.3	171	35	136	61	37	24
120	n_n=0.5	121	45	76	0		
	n_n=0.3	85	40	45	0		

Table 7. Modeling results for depths to permafrost top and base and permafrost thickness, 50 m of alternated sand and clay silt (clay) lying over bedrock, NE area

Sea depth, m	Alternating layers, 0.5 and 0.3 volumetric fraction of sand (n_n)	Geothermal heat flux, mW/m^2					
		50			75		
		Depth to base, m	Depth to top, m	Thickness, m	Depth to base, m	Depth to top, m	Thickness, m
5	n_n=0.5	214	21	193	0		
	n_n=0.3	208	21	187	0		
50	n_n=0.5	195	37	158	0		
	n_n=0.3	188	36	152	0		
120	n_n=0.5	103	43	60	0		
	n_n=0.3	95	40	55	0		

The depth to the top of continuous permafrost is most often from 20-25 m near the shore to 35-40 m at sea depths 50-80 m (Table 6). The permafrost thickness varies from 150 to 200 m in sand-clay sediments depending on lithology and sea depth. Correspondingly, the map of Fig. 8 shows typical depths to permafrost in a range of 0 to 30 m and permafrost thicknesses from 100 to 200 m. Discontinuous permafrost lies at a depth of 40-45 m and is 0 to 100 m thick.

4.2.3. Central area

The central area covers the offshore extension of the Ob', Yenisey, and Gyda rivers (C in Fig. 3; Fig. 9) in the middle between the southwestern shelf part from the northeastern one. The area was interpreted (Kulikov and Rokos, 2017) as an unfrozen zone (a talik) corresponding to paleo-estuaries and paleo-deltas of the West Siberian rivers. In our view, however, it was rather a lake-like freshwater basin that formed when ice dammed the continuing flow of the large Siberian rivers (Ob, Yenisei, Taz, etc.) during the MIS-2 glacial event. The ice dam caused flooding of the respective shelf part in different periods; the surface area and elevations of the lake table (C in Fig. 3) changed accordingly with the ice sheet contours. Therefore, our map delineates the lake by isobaths from 0 to 80 m.

The Central area is shown in the map as occupied by sporadic permafrost: sea bottom rises within its limits may be frozen (like the cases of Yamal and Ob' Gulf). In fact, permafrost patches beneath the Sartan damlake are scarce as the deposits had stored large heat resources while staying under the ice sheet for thousands of years. The sediments currently occurring within the lake limits were much warmer than the surrounding ground during MIS-2: +4 °C against -19 to -23 °C, respectively. The patches of permafrost lie at depths from 0 to 30 m and the permafrost thickness is a few tens of meters.

4.2.4. Estuary (bays)

Permafrost in the quite well documented Ob' estuary (E in Fig. 3) is restricted to a narrow strip along the shore; it is relict permafrost beneath the coast exposed to marine erosion. The total thickness of present and relict permafrost exceeds 20 m within the 1 m isobath, is no more than 10 m at sea depths between 0 and 2-3 m, and pinches out seaward in deeper water; the depth to subsea permafrost within 3 m of water depths is 5 to 15 m or more (Baulin, 2001). Coastal permafrost is traceable as far as the Cape Kamenny at 68°N (Kokin and Tsvetinsky, 2013). The patches of frozen ground are limited to a 100 m wide strip along the shore (less often 300 m).

Seismic reflection profiling reveals numerous gas reservoir zones (Rokos and Tarasov, 2007) and presumably a frozen deposits at a sea depth of 15 m at 71° N (Slichenkov et al., 2009). The estuaries (south of 71.5° N) are mapped as mainly thawed zones with near-shore permafrost at ≤3 m sea depths.

We agree with the previous inference (Melnikov et al., 1998; Badu, 2014) that permafrost within gas fields (Rusanovskaya and other gas-bearing geological structures) does not refer to relict frozendeposits. Their genesis and cryogenic age is the subject of debate.

5. Conclusions

The present state and 125 -kyr history of permafrost in the Kara shelf has been modeled with reference to the existing knowledge. Since 125 kyr ago, the parameters of permafrost have been controlled by glacial and isostatic rebound events: frozen ground is present currently in places which were free from ice but is absent from those covered by ice during the MIS-2 glacial.

Degradation of glaciation led to ice rebound and related transgression. As a result, permafrost thawed, partially after the MIS-5b cold event and completely after the MIS-4 event (during the Karginian interstadial, MIS-3).

As a result, the present shelf comprises frozen, cooled, and thawed deposits. Permafrost occurs in the periglacial domain, cooled rocks correspond to areas of MIS-2 glaciation, while thaweddeposits occupy the areas that were exposed to

485 the effect of >0 °C Atlantic waters (e.g., the western St. Anna trench) in the early postglacial time (16-15 kyr BP); thawed depositsare also found over the overwhelming part of river estuaries in northern West Siberia, except for the river mouths.

The periglacial shelf part is divided into zones of continuous, discontinuous to sporadic, and sporadic permafrost. The geocryological conditions become harsher (continuous, deep, and thick permafrost) from southwest to northeast and from large sea depths to near-shore shallow water.

490 The distribution and parameters of permafrost have had multiple controls:

(1) latitudinal climatic zonation and division into sectors;

(2) sea depths that affected the duration of regressions and transgressions and the related freezing and thawing of permafrost, respectively;

(3) an ice-dammed freshwater lake that existed during the MIS-2 event;

495 (4) geothermal heat flux;

(5) lithology and properties of deposits;

(6) sea water and seasonal ice cover that affect salinity (and hence freezing-thawing temperatures) of deposits;

(7) thermal effect from river waters.

The periglacial shelf part is divided into the southwestern, northeastern, central, and estuary areas. The 500 southwestern area comprises two subareas: a zone of discontinuous to sporadic permafrost along the shore, within 20 m sea depths in the north and 5-7 m in the south, which grades seaward into a zone of only sporadic permafrost. In the former zone, the permafrost has its table at depths from 0 to 30 m and is a few tens of meters to 100 m thick; in the latter zones, the depth to permafrost is 20 to 50 m and the permafrost thickness is less than 50 m.

In the northeastern area, continuous permafrost occurs within sea depths from 0 to 80 m and has a thickness of 505 100-200 m; the depth to its top varies from 0 to 30 m. The 80-120 m sea depth interval is occupied by ≤100 m thick discontinuous to sporadic permafrost with its table at a depth of 20-50 m.

Permafrost in the central area is sporadic; it is within 50 m thick and its top lies from 0 to 30 m deep. Deposits in the estuaries are mostly unfrozen; relict permafrost is restricted to a 100-300 m strip along the shore.

The studies performed were based on drilling and seismic acoustic data published to date. The study of the shelf 510 by drilling and geophysical methods continues. Therefore, the results of the studies performed by the authors can be used in planning new drilling and in the geocryological interpretation of seismoacoustic profiling.

Acknowledgement

The authors are grateful to all project participants in the for assistance in collecting and processing an extensive 515 amount of information from various fields of knowledge that was necessary for conducting the research and obtaining the presented results. The project was carried out by the Foundation «National Intellectual Resource» (involving experts from Moscow State University) jointly with the Arctic Research Center of the Rosneft Oil Company.

References

520

kriolog: Software for a numerical geotechnical modeling of thermophysical processes in freezing and frozen soils, available at: https://github.com/kriolog/qfrost, last access: 15 February 2020

Astakhov, V.I., Nazarov, D.V.: Late Pleistocene stratigraphy in northern West Siberia. Regionalnaya Geologiya i Metallogeniya, 43, 36-47, 2010 (in Russian).

525 Badu, Yu.B.: The influence of gasbearing structures on the thickness of cryogenic strata of Jamal Peninsula. Kriosfera Zemli, XVIII (3), 11-22, 2014 (in Russian).

Baranov, I.Ya.: Goecryological Map of the USSR. Scale 1:10 000 000. Explanatory Note. Moscow, Russia, 48 , 1960 (in Russian).

Baranskaya, A.V., Romanenko, F.A., Arslanov, Kh.A., Maksimov, F.E., Starikova, A.A. and Pushina, Z.V.: Perennially frozen deposits of Bely island: stratigraphy, age, depositional environments. Earth's Cryosphere, XXII (2), 3-15, DOI: 10.21782/KZ1560-7496-2018-2(3-15) ,2018.Bauch, H.A., Muller-Lupp, T, Taldenkova, E., Spielhagen, R.F., Kassens, H., Grootes, P.M., Thiede, J., Heinmeir, J., Petryasov, V.V.: Chronology of the Holocene transgression at the Northern Siberia margin. Global and Planetary Change, 31 (1-4), 125-139, https://doi.org/10.1016/S0921-8181(01)00116-3, 2001.

Baulin, V.V.: Engineering geological studies in the Arctic shelf: experience, results, and regulations, in: Development of the Russian Arctic Shelf, Proc. 5th Intern. Conf. RAO-01, St. Petersburg, 36-239, 2001 (in Russian).

Baulin, V.V., Ivanova, N.V., Rivkin F.M., Chernyad'ev, V.P., Shamanova, I.I.: Coastal cryolithozone of the Northwest Yamal: problems of development. Kriosfera Zemli, IX (1), 28-37, 2005 (in Russian).

Bolsiyanov, D.Y., Anokhin, V.M., Gusev, E.A.: New data on the structure of the relief and the fourth vertical deposits of the Novaya Zemlya archipelago. Geological and geophysical characteristics of the lithosphere of the Arctic region. Proceedings of VNIIOkeangeologiya, vol. 210, issue 6, 149-161, 2006 (in Russian).

Bolshiyanov, D.Y., Grigoriev, M.N., Schneider, V., Makarov, A.S., Gusev, E.A.: Late Pleistocene sealevel change and formation of an ice complex on the Laptev Sea shore, in: Basic Problems of the Quaternary: Results and Main Prospects, Geos, Moscow, 45-49, 2007 (in Russian).

Bolshiyanov, D.Yu., Pogodina, I.A., Gusev, E.A. Sharin, V.V., Aleksev, V.V., Dymov, V.A., Anohin, V.A., Anikina, N.Yu., Derevyanko, L.G.: Shorelines of the Franz Joseph Land, Novaya Zemlya, and Svalbard: New data. Problemy Arktiki i Antarktiki, 82 (2), 68-77, 2009 (in Russian).

Bondarev, V.N., Loktev, A.S., Dlugach, A.G. Potapkin, Yu.V.: Methods for studies of subsea permafrost, in: Sedimentological Processes and Evolution of Marine Ecosystems in Marine Periglacial Conditions, Apatity, vol. 1, , 15-19, 2001 (in Russian).

Bylinskiy, E.N.: Effect of Glacial Isostasy on the Pleistocene Terrane Evolution. National Geophysical Committee of the Russian Academy of Sciences, Moscow, 212, 1996. (in Russian)

Chekhovsky, A.L.: Distribution of permafrost under the Kara Sea bottom. Transactions, PNIIIS, Moscow, issue 18, 100-110, 1972(in Russian).

~~su~~Chuvilin, E.M., Perlova, E.V., Baranov, Yu.B., Kondakov, V.V., Osokin, A.B., Yakushev, V.S.: The structure and properties of cryolithozone sediments of the southern part of the Bovanenkovo gas condensate field. Geos, Moscow, 20, 2007 (in Russian).

Danilov, I.D., Buldovich, S.N.: Dynamics of permafrost related to transgressions and regressions in the Arctic basin, in: Fundamentals of Geocryology, Moscow State University, Moscow, vol. 4, 372-382, 2001 (in Russian).

Derevyagin, A.Yu., Chizhov, A.B., Brezgunov, V.S., Hubberten, Kh.-V., Siegert, K.: Stable isotope composition of ice wedges in the Sabler Cape (Lake Taimyr). Kriosfera Zemli, III (3), 41-49, 1999 (in Russian).

Dlugach, A.G., Antonenko, S.V.: Main Distribution and Structure Patterns of Permafrost in the Barents-Kara Shelf: Implications for Petroleum Exploration. AMIGE, Murmansk, 271 , 1996 (in Russian).

Dubrovin, V.A., Kritsuk, L.N., Polyakova, E.I.: Temperature, composition and age of the Kara sea shelf sediments in the area of the geocryological station Marre-Sale. Earth's Cryosphere, XIX (4), 3–16, 2015 (in Russian).

Forman, S.L., Ingolfsson, O., Gataullin, V., Manley, W., Lockrantz, H.: Late Quaternary stratigraphy, glacial limits, and paleoenvironments of the Marresale area, western Yamal Peninsula, Russia. Quaternary Research, 57, 355-370, https://doi.org/10.1006/qres.2002.2322, 2002.

Fotiev, S.M.: Formation of the major-ion chemistry of natural waters in the Yamal Peninsula. Kriosfera Zemli, III (2), 40-65, 1999 (in Russian).

Flint, R.F.: Glacial and Pleistocene geology. N.Y., J. Wiley , IV, 553 , https://doi.org/10.3189/S0022143000024060, 1957

Gavrilov, A.V.: The cryolithozone of the Arctic shelf of Eastern Siberia (current state and history of development in the Middle Pleistocene - Holocene). Dissertation for a degree. D.Sc. M., 48, 2008(in Russian).

Geinz, A.E., Garutt, V.E.: Radiocarbon (^{14}C) dating of mammoth and woolly rhinoceros fossils from Siberian permafrost. Doklady Akademii Nauk, 154 (6), 1367- 1370, 1964 (in Russian).

Gilbert, M.Th.P., Tomsho, L.P., Rendulic, S., Packard, M., Drautz, D.I., Sher, A., Tikhonov, A., Dalen, L., Kuznetsova, T., Kosintsev, P., Campos, P.F., Higham, Th, Collins, M.J., Wilson, A.S., Shidlovskiy, F., Buigues, B., Ericson, P.G.P, Germonpre, M., Gotherstrom, A., Iacumin, P., Nikolaev, V., Nowak-Kemp, M., Willerslev, E., Knight, J.R., Irzyk, G.P., Perbost, C.S., Fredrikson, K.M., Harkins, T.T., Sheridan, Sh, Miller, W., Schuster, S.C.: Whole-genome shotgun sequencing of mitochondria from ancient hair shafts. Science, 317, 1927–1930, 2007.

Gavrilov, A.V., Romanovskii, N.N., Romanovsky, V.E. and Hubberten, H.-W.: Offshore Permafrost Distribution and Thickness in the Eastern Region of Russian Arctic In: "Changes in the Atmosphere-Land-Sea System in the American Arctic". Proceedings of the Arctic Regional Centre vol. 3, edited by Igor P. Semiletov, Dalnauka, Vladivostok, 209-218, 2001 (in Russian).

Golubev, V.N., Konishchev, V.N., Sokratov, S.A., Grebennikov, P.B.: The effect of seasonal snow sublimation on the oxygen isotope composition of ice wedges. Kriosfera Zemli, 3, 71-77, 2001 (in Russian).

Grigoriev, N.F.: Coastal Permafrost in the Western Yamal Peninsula, Kn. Izdatelstvo, Yakutsk, 110 , 1987 (in Russian).

Gusev, E.A., Arslanov, Kh.A., Maksimov, F.E., Molod'kov, A.N., Kuznetsov, V.Yu., Smirnov, S.B., Chernov, S.B., Zherebtsov, I.E., Levchenko, S.B.: Late Pleistocene-Holocene sediments in the Yensei lower reaches: New geochronological data. Problemy Arktiki i Antarktiki, 2 (88), 36-44, 2011 (in Russian).

Gusev, E. A., Molod'kov, A. N. Structure of sediments of the final stage of the Kazantsevo transgression (MIS 5) in the north of Western Siberia. Doklady Earth Sciences, 443(2), 458-461, 2012

Gusev E.A., Sharin V.V., Dymov V.A., Kachurina N.V., Arslanov Kh.A.: Shallow sediments in the northern Kara shelf: New data. Razvedka i Okhrana Nedr 8, 87-90, 2012a.

Gusev, E.A., Kostin, D.A., Rekant, P.V.: Genesis of Quaternary deposits in the Barentsevo-Kara shelf (State Geological Map of the Russian Federation, scale 1:1 000 000). Otechestvennaya Geologiya, 2, 84-89, 2012b (in Russian).

Gusev, E.A., Bolshiyanov, D.Yu., Dymov, V.A., Sharin, V.V., Arslanov, Kh.A.: Holocene marine terraces of southern islands of the Franz Joseph Land archipelago. Problemy Arktiki i Antarktiki, 97 (3), 103-108, 2013(in Russian).

Gusev, E.A., Molodkov, A.N., Anikina, N.Yu., Derevianko, L.G.: Origin and age of watershed sands in the northern part of the Yenisei catchment. Proceedings of the Russian Geographical Society, 147 (4), 51-62, 2015a (in Russian).

Gusev, E.A., Molodkov, A.N., Derevyanko, L.G.: The Sopkarga mammoth, its age and living conditions (northern West Siberia). Uspekhi Sovremennogo Estestvoznaniya, 1-3, 432-435, 2015b (in Russian).

Gusev, E.A., Maksimov, F.E., Molodkov, A.N, Yarzhembovsky, Ya.D., Makaryev, A.A., Arslanov, Kh.A., Kuznetsov, V.Yu., Petrov, A.Yu., Grigoryev V.A., Tokarev, I.V.: Late Pleistocene-Holocene deposits of western Tai`myr and islands of the Kara Sea: New geochronological constraints. Problemy Arktiki i Antarktiki, 109(3), 74-84, 2016a (in Russian).

Gusev, E.A., Molodkov, A.N., Streletskaya, I.D., Vasiliev, A.A., Anikina, N.Yu., Bondarenko, S.A., Derevyanko, L.G., Kupriyanova, N.V., Maksimov, F.E., Polyakova, E.I., Pushina, Z.V., Stepanova, G.V., Oblogov, G.E.: Deposits of the Kazantsevo transgression (MIS-5) in the northern part of the Yenisei catchment. Russian Geology and Geophysics, 54 (4), 743-757, 2016b (in Russian).

Gusev, E.A., Sharin, V.V., Dymov, V.A., Kachurina, N.V., Arslanov, Kh.A,: Shallow sediments in the northern Kara shelf: New data. Razvedka i Okhrana Nedr, 8, 87-90, 2012a (in Russian).

Gutenberg B.: Changes in sea level, postglacial uplift, and mobilityof the Earth's intertor // Geol. Soc. Amer. Bull, v. 52, N 5, 251-286, 1941.

Hughes A.L.C., Gyllencreutz R., Lohne Sh.S., Mangerud J., Svendsen J. I.: The last Eurasian ice sheets – a chronological database and time-slice reconstruction, DATED-1. Boreas 45, 1–45, doi: 10.1111 (bor.12142. ISSN 0300-9483), 2016.

Kudryavtsev, V.A.(Ed.): Methods of Cryogenic Survey. Moscow State University, Moscow, 358 , 1979 (in Russian).Khrustalev, L.N., Emeliyanov N.V., Pustovoit, G.P., Yakovlev, S.V.: WARM software for calculating the thermal interaction of engineering structures with permafrost. Certificate No. 940281, RosAPO, 1994 (in Russian).

Khutorskoi, M.D., Akhmedzyanov, V.R., Ermakov, A.V., Leonov, Yu.G., Podgornykh, L.V., Polyak, B.G., Sukhikh, E.A., Tsybula, L.A.: Geotehrmics of Arctic seas. Transactions, Geological Institute, Moscow ,issue 605, , 232 ., 2013 (in Russian).

Kokin, O.V., Tsvetinskiy, A.S.: Geocryology of the Ob' Gulf slope contacting fast ice. Vesti Gazovoi Nauki, 14, 67-69, 2013 (in Russian).

Kulikov, S.N., Rokos, S.I.: Detection of permafrost in seismoacoustic time sections from shallow-water areas in the Pechora and Kara seas. Geofizicheskie Izyskaniya, 3, 34-42, 2017 (in Russian).

Lamberk, K., Chappell, J., Sea level change through the Last Glacial cycle. Science, 292 (5517), 679-686, DOI: 10.1126/science.1059549, 2001.

Leibman, M.O., Kizyakov, A.I.: Cryogenic landslides in the Yamal and Yugor peninsulas. Tipografia Rosselkhozakademiya, Moscow, 206 , 2007 (in Russian).

Levitan, M.A., Lavrushin, Yu.A., Stein R.: Deposition history in the Arctic ocean and Subarctic seas for the past 130 kyr. GEOS, Moscow, 404 , 2007 (in Russian).

Levitan M.A.: Quaternary advection of Atlantic waters into the Arctic: a review, in: Geology and Geoecology of the Eurasian Continental Margins, GEOS, Moscow, issue 1, 54-63, 2009 (in Russian).

Melnikov, V.P., Spesivtsev, V.I.: Engineering Geological and Geocryological Conditions in the Barents and Kara Seas. Novosibirsk, Nauka, 198 , 1995 (in Russian).

Melnikov, V.P., Fedorov, K.M., Wolf, A.A., Spesivtsev, V.I.: Near-bottom ice mounds in the shelf: Possible formation scenario. Kriosfera Zemli, II (4), 51-57, 1998 (in Russian).

Molodkov, A.N., Hutte, G.I., Makeev V.M., Baranovskaya, O.F., Kosmodamiansky, A.V., Ponomareva, D.P., Bolshiyanov, D.Yu.:EPR dating of mollusk shells in Oktyabrskoi Revolutsii and Kotelny islands, in: New Data on Quaternary Geochronology, Nauka, Moscow, 236-243, 1987 (in Russian).

Nazarov, D.V.: Quaternary Deposits in the Central West Siberian Arctic. Author's Abstract, Ph.D. thesis). St. Petersburg, 24, 2011 (in Russian).

Neizvestnov, Ya.V., Borovik, O.V., Kozlov, S.A., Kholmyansky, M.A.: Subsea permafrost in the Barents, Kara, and Beloye seas, in: Proc. 3rd Conf. of Russian Geocryologists,vol. 3, Moscow University, Moscow, 184-190, 2005 (in Russian).

Nikonov, A.A.: Holocene and Current Crustal Movements. Nauka, Moscow, 240, 1977 (in Russian).

Parkhomenko, S.G.: Sketch Map of Permafrost and Frost Depth in the USSR. Transactions, CNIIGAiK, issue 16, 1937 (in Russian).

Nicolsky, D. J., Romanovsky, V.E., Romanovskii, N.N., Kholodov, A.L., Shakhova, N.T., Semiletov, I.P.: Modeling sub-sea permafrost in the East Siberian Arctic Shelf: The Laptev Sea region. Journal of Geophysical Research, Issue 117, Art. no. F03028, 2012.

Pesotsky, D.G.: *Qfrost* software for geocryological modeling. Certificate of the State Registration No. 2016614404 of 22 April 2016 (in Russian).

Pogodina, I.A.: Spatial distribution and evolution of foraminiferal communities during global climate change. Vestnik Yuzhnogo Nauchnogo Centra RAN, 5 (2), 64-72, 2009 (in Russian).

Portnov, A., Mienert, J., Serov, P.: Modeling the evolution of climate-sensitive Arctic subsea permafrost in regions of extensive gas expulsion at the West Yamal shelf. Journal of Geophysical Research: Biogeosciences 119 (11), 2082-2094, doi: 10.1002/2014JG002685, 2013.

Pustovoit, G.P.: Numerical solutions / Fundamentals of Geocryology. Part 5. (Engineering geocryology), edited by: Ershov, E. D., Moscow State University, Moscow, 41-55, 1999 (in Russian).

Rokos, S.I., Dlugach, A.G., Loktev, A.S., Kostin,D.A., Kulikov, S.N.: Permafrost in the Pechora and Kara shelves: genesis, lithology, and distribution conditions. Vserossiyskiy Inzhenerno-analiticheskiy zhurnal, 10, 38-41, 2009 (in Russian).

Rokos, S.I., Kostin, D.A., Dlugach, A.G.: Free gas and permafrost in shallow sediments of the Pechora and Kara shelf areas, in: Sedimentation Processes and Evolution of Marine Ecosystems in Marine Periglacial Conditions, Book 1, KNC RAN, Apatity, 40-51, 2001 (in Russian).

Rokos, S.I., Tarasov, G.A.: Gas-saturated sediments in estuaries and gulfs in the southern Kara sea. Bull. Commission on the Quaternary, 67, 66-75, 2007.

Romanenko, F.A.: Regional evolution features of the Arctic shelf in the Holocene. Geomorfologiya, 4, 81-92, 2012 (in Russian).

Romanovskii, N.N., Hubberten, H.-W., Gavrilov, A.V., Eliseeva, A.A., Tipenko, G.S. Offshore permafrost and gas hydrate stability zone on the shelf of East Siberian Seas. Geo-Marine Letters, v. 25, N 2-3, p. 167-182, 2005 (in Russian).

Romanovsky, N.N., Tumskoy, V.E.: Retrospective approach to the assessment of the modern distribution and structure of the shelf cryolithozone of the Eastern Arctic. Earth's Cryosphere, vol. XV, issue. 1, p. 3-14, 2011 (in Russian).

Siddall, M., Rohling, E. J., Almogi-Labin, A., Hemleben, Ch., Meischner, D., Schmelzer, I., Smeed, D.A.: Sea-level fluctuations during the last glacial cycle. Nature 423, 853-858, https://doi.org/10.1038/nature01690, 2003.

Siddall, M., Chappel, J., Potter, E.K.: Eustatic sea level during past interglacials, in: Sirocko, F. et al. (Eds.), The Climate of Past Interglacials. Elsevier, Amsterdam, 75 – 92, 2006.

Slichenkov, V.I., Samoilovich, Yu.G., Nikolaev, V.V., Konstantinov, V.M.: Structure of Cenozoic sediments in the northern Ob' gulf, Kara Sea; evidence from acoustic data. Problemy Arktiki i Antarktiki, 82 (2), 106-117, 2009 (in Russian).

Stein, R., Val, K., Polyakova, E.I., Dittmers, K., Postglacial changes in the river runoff and deposition environments in the southern Kara sea, in: The System of the Laptev Sea and Adjacent Arctic Seas. Current State and Evolution. Moscow State University, Moscow, 410-426, 2009 (in Russian).

Streletskaya, I.D., Shpolanskaya, N.A., Kritsuk, L.N., Surkov, A.V.: Cenozoic deposits in the Yamal Peninsula and the problem of their origin. Vestnik Moscow University, ser. 5, geography 3, 50-57, 2009 (in Russian).

Streletskaya, I.D., Gusev, E.A., Vasiliev, A.A., Rekant, P.V., Arslanov, Kh.A.: Late Pleistocene-Holocene ground ice in Quaternary deposits on the Kara shelf as a record of paleogeographic conditions. Bulletin of the Commission on Quaternary, 72, 28-59, 2012 (in Russian).

Streletskaya, I.D., Vasiliev, A.A., Oblogov, G.E., Tokarev, I.V.: Reconstruction of paleoclimate of Russian Arctic in Late Pleistocene–Holocene on the basis of isotope study of ice wedges. Earth Cryosphere, XIX (2), 98–106, 2015 (in Russian).

Sulerzhitsky, L.D., Tarasov, P.E., Andreev, A.A., Romanenko, F.A.: The Upper Quaternary pollen-based stratigraphy of Sverdrupp Island. Stratigrafiya. Geologicheskaya Korrelatsiya, 3 (2), 98-104, 1995 (in Russian).

Svendsen, J., Alexahderson, H, Astakhov, V., Demidov, I., Dowdeswell, Ju., Funder, S., Gataulin, V., Henriksen, M., Hjort, H., Houmark-Nielsen, M., Hubberten, H.-W., Ingolfsson, O., Jakobsson, M., Kjar, K, Larsen, E., Lokrantz, H., Lunkka, Ju.P., Lysa, A., Mangerud, J., Matiouchkov, A., Murray, A., Moller, P., Niessen, F., Nikolskaya, O., Polyak L., Saarnisto, M., Siegert, Ch., Siegert, M., Spielhagen, R., Stein, R.: Late Quaternary ice sheet history of northern Eurasia. Quaternary Science Reviews, 23, 1229-1271, https://doi.org/10.1016/j.quascirev.2003.12.008, 2004.

Shishkin, M.A., Faibusovich, Ya.E., Shkarubo, S.I., Nazarov, D.V., Abakumova, L.A., Borozdina, Yu.A., Voronin, A.S., Gerasicheva, A.V., Gorelina, T E., Zavarzina, G.A., Zinchenko, A.G., Zuikova, O.N., Kostin, D.A., Lang, E.I., Likhotin, V.G., Markina, T.V., Petrov, S.Yu., Petrova, M.N., Cannon, D.V., Radchenko, M.S., Rubin, L.I., Seregin, S.V., Solonina, S.F., Sychev, S.N., Tortsov, Yu. I., Bazhkova, S.F., Vasilenko, E.P., Ivanova, E.I., Perlov, D.K., Ruchkin, M.V., Stepanova, A.P.: The State Geological Map of the Russian Federation Scale 1:1000000 (third generation). Ser. West Siberia, Sheet R-42, Yamal Peninsula, Explanatory note. Saint Petersburg, VSEGEI, 2015 (in Russian).

Trofimov, V.T. (Ed.), Badu Yu.B., Kudryashov V.G., Firsov N.G.: The Yamal Peninsula (Engineering-Geological Review). Moscow State University, Moscow, 278 , 1975 (in Russian).

Ushakov, S.A., Krass, M.S.: Gravity and Mechanics of the Earth's Interior. Nedra, Moscow, 157, 1972 (in Russian).

Vasiliev, A.A., Rekant, P.V., Oblogov, G.E., Korostelev, Yu.V.: A new GIS–oriented map of subsea permafrost in the Kara Sea, in: Proc. Session of Scientific Council on Geocryology. Russian Academy of Sciences, vol. 1, 291-295, 2018 (in Russian).

Vasil`chuk, Yu.K.: Oxygen Isotope Composition of Ground Ice: An Experience of Geocryological Reconstructions. Mosobluprpoligrafizdat, Moscow, Book 1, 420 Book 2, 264 pp., 1992 (in Russian).

Vasil`chuk, Yu.K., Serova, A.K., Trofimov, V.T.: Deposition environment of Karginian sediments in northern West Siberia. Bull. Commission for Quaternary, 53, 28-35, 1984 (in Russian).

Volkov, N.G.: Prediction of Temperature and Major-Ion Chemistry of Pore Water in Saline Permafrost and Cryopegs: Case Study of the Yamal Peninsula). Author's Abstract, Ph.D. thesis, Moscow, 26 , 2006 (in Russian).

Yershov, E.D.(Ed.): Geocryological Map of the USSR, scale 1:2 500 000. Moscow State University, Moscow, 1991 (in Russian).

Yershov, E.D. (Ed.):: Geocryology of the USSR. West Siberia. Nedra, Moscow, 454, 1989 (in Russian).

Yershov, E.D. (Ed.):: Fundamentals of Geocryology. Part 4. Dynamic Geocryology. Moscow State University, Moscow, 688, 2001 (in Russian).

Zastrozhnov A.S., Shkatova V.K., Minina E.A., Tarnogradsky V.D., Astakhov V.I., Gusev E.A.:Map of Quaternary deposits in the Russian Federation, scale 1:2 500 000, Explanatory note. Saint Petersburg, VSEGEI, VNII Okeangeologiya, 2010 (in Russian).